HYDROPHILIZATION OF POLYSULPHONE ULTRAFILTRATION MEMBRANES BY POLAR POLYMERIC SOLUTE INCORPORATION

EP Jacobs • SP Roux • M Meinchen •
AJ van Reenen • CE Morkel

WRC Report No. 1268/1/06

Water Research Commission

Hydrophilization of Polysulphone Ultrafiltration Membranes by Polar Polymeric Solute Incorporation

Report to the
WATER RESEARCH COMMISSION

by

EP Jacobs
SP Roux
M Meinchen
AJ van Reenen
CE Morkel

Dept of Chemistry & Polymer Science
University of Stellenbosch
Stellenbosch

WRC Report 1268/1/06
ISBN No: 1-77005-478-2

NOVEMBER 2006

Executive summary

Rationale

Membranes foul as result of the filtration operation and by nature of the membrane material of construction. Polysulphone (PSU) is the thermoplastic material of choice for the manufacture of various types of ultrafiltration (UF) membranes. This material increases the robustness of membranes due to its structural- and chemical stability. Unfortunately PSU is a hydrophobic material, with a relatively low surface energy and high water contact angle, and membranes made from such material are more vulnerable to adsorptive fouling. In order to capitalize on the usefulness of PSU membranes in filtration operations, chemical modification of this material to make it more polar and less hydrophobic was at the core of this study**.**

Various techniques and approaches to introduce polarity on the exposed structure of PSU membranes have been studied and developed by others to impart hydrophilicity. Excellent results have been achieved with flat-sheet membranes using surface modification techniques such as plasma coating and photo-induced grafting to improve PSU membrane wettability. Unfortunately these techniques are not amenable to the capillary membranes used in this study and a different approach had to be adopted.

Aims

In order to develop a membrane with better fouling resistance, a research project with the following initial aims were entered into:

- produce hydrophilic, non-fouling, UF membranes by means of in-situ coating of existing membranes;
- produce hydrophilic, non-fouling membranes by incorporating the hydrophilizing polymers into the membrane materials during the manufacturing process;
- produce high molecular mass cut-off hydrophilic capillary and tubular membranes to extend the range of available product for use in potable water production and the treatment of high-fouling effluents; and
- perform bench-scale studies with model and real effluents to compare the performances of current capillary and tubular UF membranes with hydrophilized membranes originating from this project.

Method approach

The main aim of the project was to develop a technique to improve the fouling resistance of PSU UF membranes. Various options are available. However, not all of them are applicable to tubular-type membrane geometries, such as the capillary membranes developed during this project. Coating is a simple hydrophilization approach. However, surface coating has two drawbacks. First, coating impairs membrane flux performance in that the coating material acts as a preferential fouling layer. The negative impact that surface coating has on membrane flux makes this approach less attractive. Second, the coating layer desorbs with time, resulting in the membrane losing its initial hydrophilic character. In fact, an alkaline detergent wash is a hydrophilization process in itself but its effects do not last long. A better approach was to coat the membranes with an amphiphilic polymer, such as Pluronic. Pluronic, a di-block copolymer of poly(ethylene oxide) and poly(propylene oxide) does not desorb readily and its hydrophilization effect lasts longer, but at the cost of a 40% reduction in initial membrane pure-water permeability flux.

So, the underlying idea in this study was to impart a more permanent hydrophilic character to the membranes by synthesizing a polymeric compound which is compatible with the membrane

polymer in solution, but which is not soluble in the non-solvent (water) in which the nascent membrane is precipitated during manufacture. Because this amphiphilic compound is not water-soluble, it will not leach out of the membrane body during operation either, leading to a greater permanency of the effect of hydrophilization.

Findings

Synthesis of a suitable material, a block copolymer of poly(ethylene oxide) (PEO) and polysulphone (PSU) was accomplished with success. The PEO segments of the polymer are polar and impart hydrophilicity to the membrane. The PSU segments of the synthesized polymer are similar in chemical character to that of the PSU membrane material. This ensures thermodynamic compatibility between the synthesized material and the membrane material both in solution and solid phase. PEO is one of those rare polymers that mix homogeneously with PSU in all proportions, without incurring spontaneous phase separation. In fact, PEO as such is used in membrane formulations to induce membrane porosity because it leaches out during membrane fabrication, leaving microscopic cavities in its wake.

The research was successful in that all analytical techniques used to study treated membranes showed greater hydrophilicity compared to control membranes that did not contain the modifying material. Scale-up of the synthetic reaction was also successful according to NMR studies, and quantities of up to 5kg were synthesized at a time.

A new, high-flux capillary UF membrane was developed up to the point of entering into a membrane performance optimization study with the synthesized hydrophilizing agent as additive to the formulation. The developed membrane has merit for use in drinking water applications and in protein separation.

Because of time constraints, the work stopped short of evaluating the synthesized material as an additive to formulations from which tubular membranes are prepared. During experimentation, flat-sheet non-porous films and porous membranes were used to analyze and evaluate the hydrophilization technology under development. These flat-sheet membranes and non-porous films were cast onto non-woven spun-bonded fabric. The same support fabric is also used to prepare the support tubes used in tubular membrane fabrication. Tubular membranes are prepared by depositing a film of the membrane solution on the inside of the tubular support structure. By analogy, if polarity could be imparted to the flat-sheet structures prepared, the same polar properties could be imparted to tubular membranes if the casting and post-treatment operations were similar.

Recommendations

It is recommended that the research be furthered to:

- study the effect that the addition of the modifying agent has on membrane morphology and performance in general;
- alternative annealing practices to reduce the duration of the annealing step; and
- include tubular membranes that are manufactured in RSA based on earlier WRC technology.

Oil water separation was successfully conducted with locally produced capillary membranes, but fouling of the membranes resulted in reduced membrane flux. The hydrophilized membranes should be evaluated for usefulness in oil water separation, amongst other industrial applications.

Acknowledgements

The research team would like to express their sincere thanks to:

the Water Research Commission (WRC) of South Africa who funded this project;

the Centre for Macromolecular Chemistry and Technology in Tripoli/Libya for loan of the Veeco Multimode SPM that proved invaluable to the research; and

the Steering Committee, who consisted of the persons named below, for their individual contributions:

Dr G Offringa (chairman)	Water Research Commission
Prof EP Jacobs (project leader)	Dept. of Chemistry & Polymer Science, US
Prof SM Bradshaw	Dept. of Chemical Engineering, US
Mr J Parsons	Rand Water
Prof SF Mapolie	Dept. of Chemistry, UWC
Dr JJ Schoeman	Water Utilities Group, PU
Mr GT Burch	Mondi
Mr JG Nieuwenhuis	SASOL
Dr AJ van Reenen	Dept. of Chemistry & Polymer Science, US
Mr OCE Hempel (secretary)	

Dr Gerhard Offringa on his challenge, after a meeting on severe fouling of tubular UF membranes operating on a pulp & paper effluent, to come up with a membrane that fouls less;

Dr Albert van Reenen for valuable input with respect to polymer synthesis and characterization and for acting as promoter for Charl Morkel and co-promoter for Stephan Roux;

Dr Martina Meincken who helped to set new AFM measurement standards;

Charl and Stéphan who conducted the basic research; and

Deon Koen who spun the membranes.

List of abbreviations

AFM	Atomic force microscopy
HRP	Horseradish peroxidase
NMP	N-methyl, 2-pyrrolidone
PEO	Poly(ethylene oxide)
PSU	Polysulphone
PVP	Poly(vinyl pyrrolidone)
PWF	pure water flux
PWF_{60}	Pure water membrane flux determined after 60 min

Table of contents

List of figures

List of tables

1. Introduction

Membranes foul as a result of the nature of the filtration operation and by nature of the membrane material of construction.

Concentration polarization occurs because solutes that are retained by the membrane accumulate at the membrane surface until their convective flow towards the membrane interface is balanced by their diffusive flow back into the bulk of the feed stream. This fouling is not necessarily permanent, because its effect on flux can be reduced by choice of operating protocol. Adsorptive fouling, on the other hand, is more permanent. In the latter case foulants cause more permanent bridging and blinding of pores, and chemical cleaning to displace these foulants is the only way to restore membrane flux performance. In general, fouling leads to an improvement in the retention performance of fouled ultrafiltration (UF) membranes, but impairs flux performance.

How easily or how permanently the fouling manifests itself is largely dependent on the membrane material, membrane surface properties (including surface energy, topography, pore morphology, etc). Another aspect of membrane fouling concerns membrane process operation (reduction of concentration polarization), but that does not form part of this study.
If the difference in the surface-energy between the exposed membrane surface and that of water can be reduced, increased wetting of the membrane will occur, reducing the propensity of components in the water to fix themselves at adsorption sites on the membrane surface and within pores. Therefore, the greater concentration levels of contaminants at the membrane surface that results from concentration polarization will have fewer propensity to adsorb onto exposed surfaces of the membrane and mechanical means of flux restoration will be more effective.

Polysulphone (PSU) is the thermoplastic material of choice for the manufacture of various types of UF membranes. This material increases the robustness of membranes due to its structural- and chemical stability [1-3]. Unfortunately PSU is a hydrophobic material, with a relatively low surface energy and therefore a high water contact angle. This means that water does not wet the surface of the material and that membranes made from such materials are more vulnerable to fouling through adsorptive mechanisms. In order to capitalize on the robustness of PSU in filtration applications, chemical modification of this material to make it less hydrophobic is the focus of much study [4].

Various techniques and approaches to hydrophilize PSU membranes by introducing polarity on the exposed structure of such membranes have been developed [1,5]. Although excellent results have been achieved with surface modification techniques such as plasma coating and photo-induced grafting to improve membrane wettability, these techniques are not easily amenable to capillary membranes.

Capillary membranes are narrow-bore tubular-type membranes with typical outside diameters of 1 to 3mm and inside diameters of 0.7 to 1.5mm. These membranes are self-supporting and may be operated from the inside-out, or outside in. In the former case the membrane skin layer is on the inside. The feed solution is passed under pressure through the lumen of the membrane and water permeates from the inside to the outside, hence inside-out filtration. It is therefore very difficult to perform continuous radiation-type chemical reactions to modify the filtration surface of inside-out membranes (Figure 1).

Another approach to increase the polarity of a membrane is to add hydrophilizing polymeric additives, such as linear flexible poly(ethylene oxide) (PEO) or poly(vinyl pyrrolidone) (PVP) to the membrane formulation. Not all of these polymers will diffuse out of the membrane structure during membrane formation, because of entanglement with the membrane-forming polymer material. Because both PEO and PVP are polar, they give rise to higher surface energies and therefore greater membrane wettability. The net result is surface hydrophilization with a concomitant reduction in contaminant adsorption. However, hydrophilization, in this case, is a statistical event and very dependent on whether the PEO or PVP remains trapped within the membrane matrix. The more open-porous the membrane is, the better the chances are that the linear-flexible PEO will diffuse out of the membrane matrix during the membrane formation and post-treatment steps, resulting in a reduction of the potential wettability properties of the membrane.

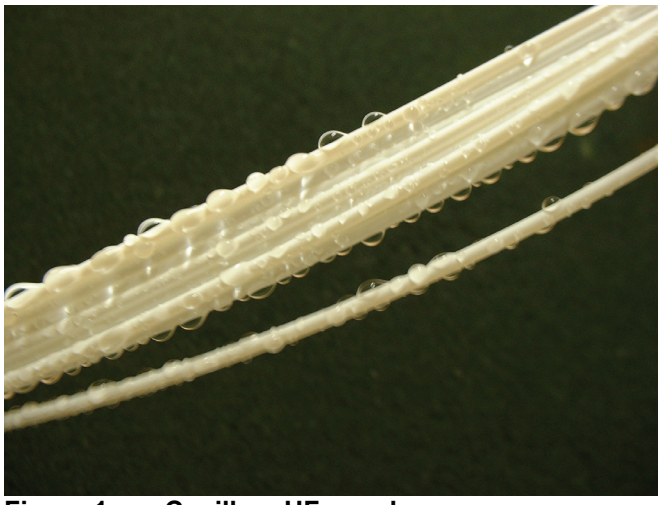

Figure 1: Capillary UF membranes.

The approach adopted in this project was rather to synthesise a new polymeric additive that contains a large percentage of PEO (a water-soluble polymer), but where the synthesized additive is only soluble in aprotic solvents such as N-methyl, 2-pyrrolidone (NMP), a solvent for the membrane-forming polymer, PSU [1,5]. Although polymer-polymer compatibility in solution is rare, PEO is an exception and is compatible with PSU in all ratios. The model polymer additive decided on was a branched PEO-PSU copolymer, where the polar PEO segments confer a more hydrophilic character to the PSU membrane surface, with the PSU segment of the macromolecule being compatible with the PSU membrane matrix. In this way a homogeneous membrane-forming solution can be prepared and the PEO-co-PSU additive will remain in the polymer-rich phase during the membrane-forming phase-inversion step.

The development of the membrane polymer-additive included the study of various synthetic routes to produce tri-block and branched PEO-block-PSU copolymers. The earlier work on tri-block copolymer synthesis will not be reported on in this document. This report therefore pertains only to aspects relating to the synthetic route developed to produce the branched block copolymer and the development of a membrane making use of the modifying additive. The synthetic route decided on was a two-step, aromatic nucleophilic substitution reaction. The resulting branched copolymer product is amphiphilic with the PEO providing the hydrophilic segments and PSU the hydrophobic segment [1].

During the wet-phase inversion membrane manufacturing process, the amphiphilic nature of the branched PEO-block-PSU copolymer favours surface segregation. PEO segments arrange at the surface of the polymer-rich phases (the phase that eventually solidifies to form the membrane bulk), which is in intimate contact with the polymer-poor phase (which eventually forms the membrane pores or porosity within the membrane bulk). This is because of the solubility of PEO in the aqueous coagulant (water). The linear block segment (PSU) of the copolymer partitions to the polymer-rich (organic) phase because of its poor solubility in water. This association of the PSU block of the copolymer with the polymer-rich phase of the nascent membrane anchors the branched surface-modifying block (PEO) to what becomes the bulk membrane matrix. This function is important to the mechanical stability of the surface-modified membrane and its stability in aggressive environments.

Advantages when using this method for membrane modification include the homogeneous modification of both internal- and external membrane surfaces during the phase inversion membrane-formation process. This is achieved by simply blending the modifying agent into the membrane formulation. The covalent linkage between the hydrophilic-branched PEO block and the hydrophobic PSU block allows the preservation of membrane surface integrity during use and avoids problems associated with slowly desorbing adsorbates and loss of initial hydrophilization in the latter case [1,5].

In this report the chemistry of the technology developed to improve membrane wettability is discussed, as well as the physical properties of modified (with polymer additive) and unmodified flat-sheet PSU films. Control UF capillary membranes (unhydrophilized) were developed during the course of the project. The preparation of these UF membranes is discussed and results of their performance on a proteinaceous feed solution are also reported on.

2. Experimental (materials and methods)

The techniques used to prepare planar membrane films and capillary membranes are described below. All surface studies were performed on dense flat-sheet membrane films. The capillary membranes that evolved during the course of the work were tested against a model protein using a readily available enzyme.

2.1 Membrane preparation and performance evaluation

Membrane solutions contain dissolved gas. The concentration of dissolved gas may be higher than the equilibrium concentration at prevailing ambient conditions, because air may also be introduced into the solution during the make-up process. Any entrapped or dissolved air can lead to the formation of imperfections in the membranes. In order to reduce the concentration of dissolved gas, all membrane formulations were heated to 40°C and evacuated overnight prior to use.

2.1.1 Flat-sheet membranes

Small sections of flat-sheet membranes were hand-cast on either plate glass or non-woven fabrics by means of an applicator blade (Figure 2). The applicator blade was in the form of a brass bar with a recess of 150 µm accurately machined to a width of 100 mm. This machined recess dictated the thickness of the nascent membrane.

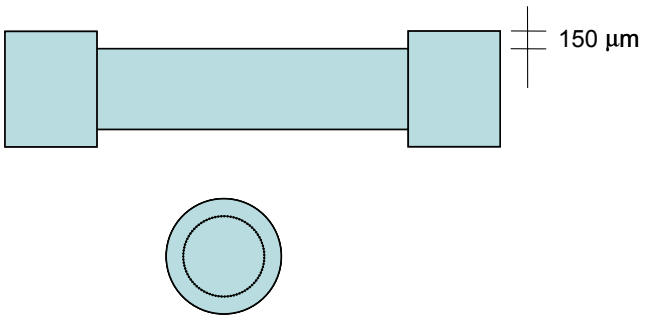

Figure 2: Spreader bar used to prepare planar membranes.

To cast a membrane film a portion of the solution was poured carefully on the glass plate or on non-woven spun-bonded fabric. This solution is then evenly spread across the receiving surface by means of the spreader bar (Figure 3). Care must be taken to avoid air-bubble intrusion when the solution is decanted from the container, or spread across the receiving surface. After a predetermined period of air-exposure, the glass plate was immersed into a bath containing a non-solvent for the polymer. This initiates the phase-inversion process that leads to the formation of a porous membrane film. The non-solvent used was usually water, sometimes containing additives. The membranes were left in this bath to allow out-diffusion of solvents from the membrane film.

When the membrane was cast on a glass plate, the membrane would release spontaneously from the plate after a short period. The membrane was then removed and further leaching was conducted in a container where the water was continuously replenished with fresh reverse osmosis filtered tap water. The membranes were stored in a solution containing a 0.1%m/m solution of sodium azide to prevent bacterial action. When the membrane was cast on a support fabric, the membrane would not peel loose and the resultant membrane composite would be removed for further leaching to remove all soluble components.

It is important to note here that when the nascent membrane is brought into contact with the non-solvent coagulation liquor, the top surface of the membrane comes into immediate contact with the coagulant. The bottom surface is initially protected from non-solvent intrusion. This results in different phase-inversion pathways with concomitant different top and bottom membrane surface structures. (This will be elucidated later in the report).

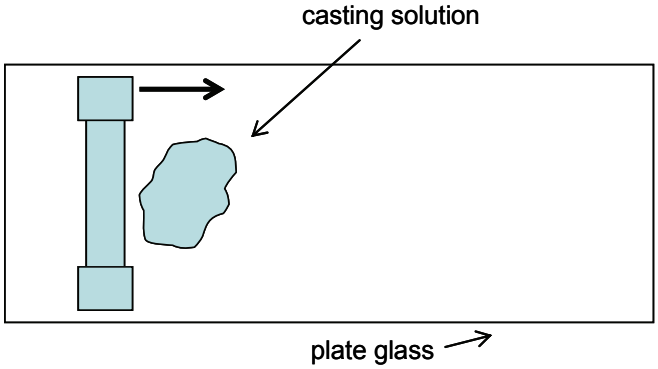

Figure 3: Technique used to prepare planar membranes from solution.

Typical formulations used during the study include those given in Table 1. (Membranes will be identified in the text by means of the code listed in the table below. The * used with the membrane code denotes that the membrane formula did not contain pore-forming agents. This allowed the preparation of non-porous polymer films with more smooth surfaces for analytical procedures).

Table 1: Typical planar membrane formulations

Membrane code	NMP % (m/m)	PSU % (m/m)	Branched PEO-block-PSU copolymer % (m/m)	PEG_{200} % (m/m)	PVP_{30K} % (m/m)	H_2O % (m/m)
Type #A	56	24	0	20	0	0
Type #B	53	24	3	20	0	0
Type #C	50	24	6	20	0	0
Type #H	50	24	0	25	0	1
Type #K	49.5	12	12	25	0.5	1

The chemicals used included the following: NMP (BASF Corporation, USA); PSU (Udell NT 3500, USA); PEG_{200} (Pluriol E200, BASF Corporation, USA); polyvinylpyrrolidone ($PVP_{30000,}$ BASF Corporation, USA) and demineralized water.

2.1.2 Capillary membranes

Capillary membranes are formed in essentially the same way as planar membranes. As in the case of planar membranes, the membrane solution is first shaped into the desired form. In order to spin a capillary membrane the membrane solution was extruded through a spinning die (spinneret), which has a needle-within-needle form (Figure 4). The solution passes through the annulus, thus forming a liquid tube. In order to achieve this, the spinning solution has to have a minimum viscosity. Viscosity is not that important in the case of planar membranes.

In order to prevent the nascent capillary membrane from collapsing, a non-solvent for the membrane polymer is metered through the inside needle and into the bore of the membrane. The inside surface of the membrane gels on contact with this fluid to form the active membrane skin layer that imparts the characteristic retention and flux performance of the

membrane. After a specified period of air contact, the outside of the membrane enters into the external coagulation bath that consisted primarily of RO filtered tap water.

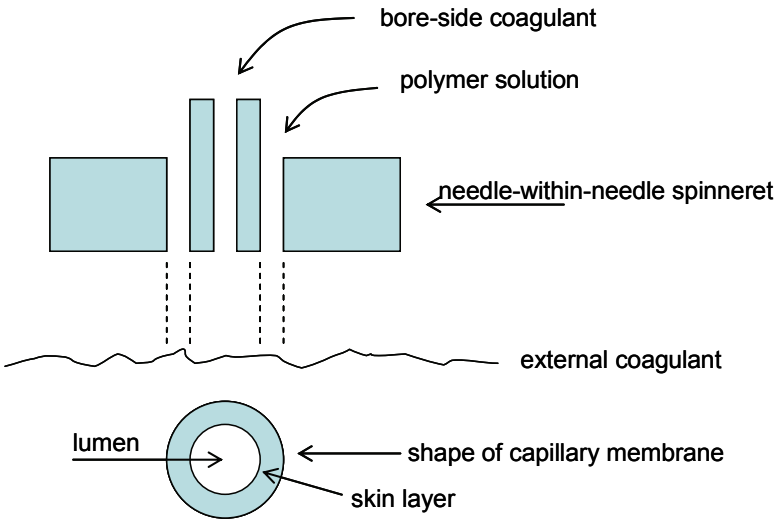

Figure 4: Illustration of the capillary membrane extrusion process.

The spinning process is continuous and after a certain period of exposure to the coagulation fluids the membrane is wound up on a take-up drum from which it is removed for further processing. Further processing steps included extended leaching, solvent exchange, and drying. The capillary membranes were normally stored dry, as opposed to wet as is the case with planar membranes. However, some of the capillary membranes were stored wet for control purposes and analysis.

Table 2: Typical capillary membrane formulations used in the study

Membrane code	NMP % (m/m)	PSU % (m/m)	PEG_{200} % (m/m)	PEG_{400} % (m/m)	PEG_{600} % (m/m)	PVP_{30000} % (m/m)	PVP/VA % (m/m)	H_2O % (m/m)	$LiNO_3$ % (m/m) of total mass
Type #D	49	24	25	0	0	0	0	2	0
Type #P	49.5	24	25	0	0	0.5	0	1	0
Type #J	49.5	24	25	0	0	0.5	0	1	0.5
Type #L	49.5	24	25	0	0	0	0.5	1	0
Type #M	49.5	24	0	25	0	0.5	0	1	0
Type #N	49.5	24	0	0	25	0.5	0	1	0

2.1.3 Membrane performance evaluation

Both flat-sheet- and capillary membranes were tested for pure water flux (PWF). The membranes were fitted into specially designed pressure cells in the case of the flat-sheet membranes or a miniaturized pressure-vessel in the case of the capillary membranes. Deionized water was used in all tests. The flat-sheet- and capillary membrane test cells were inserted into the appropriate test systems and the membrane flux was determined after 60 min of filtration time at 100 kPa (PWF_{60}). Both permeate and retentate flow was measured by weighing and the flux was determined for the specific membrane surface area involved in each case. Flux data is presented as litres per metre square surface area per hour operating time (L/m^2h).

A number of capillary membranes of a specified length were bundled and epoxied into stainless sleeves at both ends of the bundle. These were then inserted and sealed in the test cell for evaluation. A typical test loop is illustrated in Figure 5. The membranes were typically evaluated for pure-water flux at a trans-membrane pressure of 100 kPa. The retention capabilities of the membranes were routinely determined by challenging the

membranes with a 0.5% m/m solution of poly(ethylene glycol) (PEG) with a molar mass of 35kD (PEG_{35K}) at the aforesaid pressure.

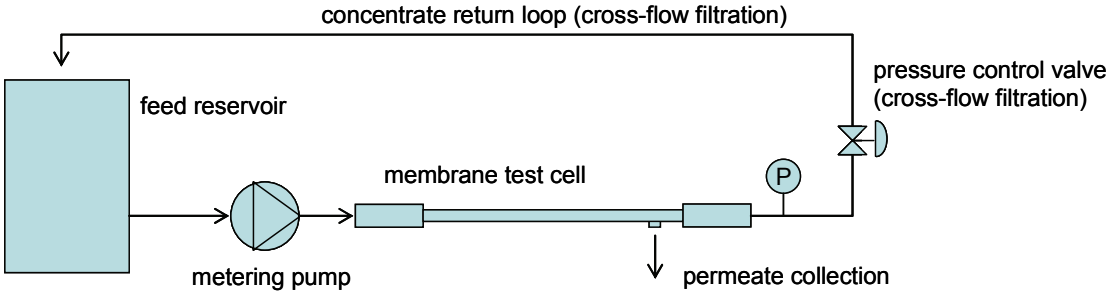

Figure 5: Typical capillary membrane test loop. The pressure control valve is shut under conditions of dead-end filtration.

PEG_{35K} retention determination

A 0.5%m/m solution PEG_{35K} (Merck-Schuchardt, Germany) is filtered through the test membrane for 60 min at 100 kPa. The permeate flow was determined and the flux of each specific membrane calculated. Samples (25 mL) of both permeate and feed solutions were collected and placed in a pre-weighed, dry glass beaker. These samples were dried by evaporation at 40 ˚C and weighed to 4-decimal places (Mettler AE200) until a constant mass was achieved. From these results the content of PEG in the permeate was determined as a percentage of the total PEG content in the feed solution. No corrections were made for concentration polarization and the retention results are reported as apparent retention (R_a).

$$R_a = \frac{1 - \text{Mass}_{\text{solute permeate}}}{\text{Mass}_{\text{solute feed}}} \times 100\ \%$$

Horseradish peroxide retention determination

Horseradish peroxide (HRP) was used as the model protein adsorbate because of its propensity to adsorb onto PSU. The retention determination is made by using a 100mg/L feed solution of HRP. The permeate was collected separately and the retentate returned to the feed solution until a desired level of concentration was achieved in the feed vessel (the so-called feed-and-bleed method of cross-flow filtration). Samples collected include the HRP solution prior to filtration, the permeate and the final concentrate. The guaiacol peroxidase assay [7] was used to determine the enzyme activity in the samples collected, which allows the determination of the membrane retention properties with respect to HRP.

Guaiacol peroxidase assay

The test principle is based on the rate of decomposition of hydrogen peroxide by the peroxidase enzyme with guaiacol as the hydrogen donor. The rate of colour development was measured spectrophotometrically at 436nm and 25ºC. The reagents include monobasic potassium phosphate, dibasic potassium phosphate, hydrochloric acid, sodium hydroxide solution, guaiacol, hydrogen peroxide and horseradish peroxidase standards.

Preparation of the solutions

Potassium Phosphate buffer (0.1M, pH 7)

Dissolve 0.53 g KH_2PO_4 (Mr 136.09) and 1.06 g K_2HPO_4 (Mr 174.18) in distilled water, adjust pH to 7 and dilute to 100 mL. Store diluent on ice and equilibrate buffer at 25ºC. The suppliers of chemicals are listed in Table 3.

Guaiacol (0.018M)

Dissolve 22.3 mg guaiacol in 10 mL water and store on ice.

Substrate
Dilute 0.1 mL 30% hydrogen peroxide with distilled water to 120 mL and adjust A_{240} (Absorbance) in 1cm light path to 0.40 to 0.41. Store on ice.

Table 3: List of chemicals used and suppliers

Materials	Abbreviation	Grade	Supplier
horseradish peroxidase	HRP	industrial	Seravac (Pty) Ltd, RSA
dibasic potassium phosphate	KH_2PO_4	CP	Merck Laboratory Supplies, RSA
Monobasic potassium phosphate,	K_2HPO_4	CP	Merck Laboratory Supplies, RSA
Guaiacol			Merck Laboratory Supplies, RSA
hydrogen peroxidase	H_2O_2	CP	Merck Laboratory Supplies, RSA
hydrochloric acid	HCl	CP	Merck Laboratory Supplies, RSA

2.1.4 Preparation of samples and standards
Dissolve 5 mg enzyme/mL in ice-cold buffer immediately before assay, dilute to yield 0.2 μ/mL with ice-cold buffer (ΔA/min of approx. 0.040 to 0.045).
Procedure
Into a quartz cuvette, pipette the following:

Buffer	2.80 mL
Guaiacol	0.05 mL
Substrate	0.05 mL
Equilibrate at 25ºC and monitor ΔA/min.	
Enzyme at time zero	0.10 mL
	3.00 mL

Evaluation for enzyme activity units (U)/mg material

$$\text{U/mg material} = \frac{\Delta A/\text{min} \times 3 \times 4 \times \text{dilution}}{2.5 \times 0.1 \times \text{mg enzyme/mL original solution}}$$

2.2 Equipment to produce branched PEO-block-PSU copolymer

2.2.1 Laboratory equipment
In order to synthesize the initial small quantities of the branched, PEO-block-PSU copolymer required to establish a synthetic route, standard laboratory equipment (Figure 6) was used as described by Hancock *et al*. [1,6,8,9]. The proper practical procedures are described later in the text. The only significant change to the method described by Hancock *et al.* [6] was the use of N_2 to purge instead of argon to reduce costs.

2.2.2 Upscale reactor to produce branched PEO-block-PSU copolymer
To produce larger quantities of the membrane-modifying copolymer, as well as to test the use of industrial type equipment for this purpose, a larger reactor system was designed and constructed (Figure 7).

The system consisted of two jacketed vessels, each with a capacity of 5 L, an oil heating system and large overhead stirrer motors. Large Dean-Starke traps were manufactured and a screw-in type fitting was designed to inject N_2 gas at the bottom of each reactor vessel. The overhead stirrer motors were connected to a stirrer shaft entering each reactor from above through a mechanical seal. This seal was filled with mercury and topped up with silica oil. The system's oil reservoir was vented to the atmosphere to avoid pressure build-up of the heating oil.

Figure 6: Laboratory equipment used for the synthesis of the first samples of the branched PEO-block-PSU copolymer. A network of cooling- and gas lines, the heating mantles and overhead stirrers as well as stirring motors mounted in a fume hood allows little free-work space. Such a system can only be expanded with difficulty and at high cost.

The original design and initial reactor system manufactured were by no means perfect. Unfortunately, the process of correcting some of the major faults regarding the proper operation of this system caused time delays. Commissioning the reactor involved many trial runs using only solvent in the reactors, as well as a fair number of actual reaction mixtures that failed to produce the desired product. Solving these problems proved expensive, but the final reactor system proved to be both reliable and capable of producing large quantities of the required copolymer according to specification. This showed that further scale-up should not be much of a technical hurdle if proper vapour seal would be installed to prevent vapour leakage at the high operating temperature. The oil heating system was far more reliable and accurate than the heating mantles used during the laboratory scale synthesis.

2.3 Description of hydrophilizing agent synthesis

The ensuing paragraphs detail the method used during the scaled-up synthesis of the hydrophilizing branched-block copolymer agent. In the approach used, a PSU and branched PEO pre-polymer are prepared first, after which they are combined to render the branched PEO-block-PSU copolymer in a further chemical reaction step.

The synthetic steps described below provided larger quantities of the hydrophilizing agent that was necessary to produce capillary membranes. The approach described below does not differ from the synthetic work-up developed to prepare smaller quantities of the material for use in flat-sheet membrane studies. The only difference was the size of the equipment used and quantities of starting materials.

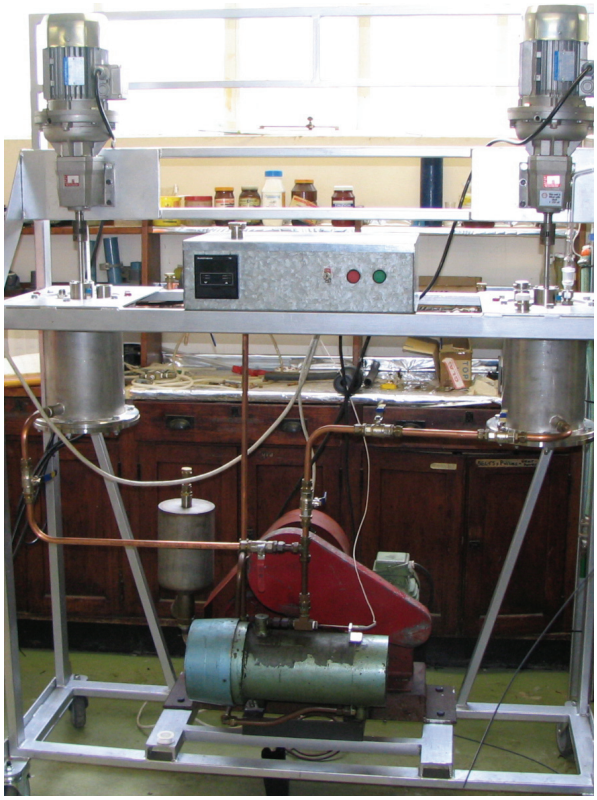

Figure 7: **The reactor system with its oil heating system proved far more reliable in heating and maintaining the proper temperature. The small oil reservoir (silver cylinder below reactors) was later replaced with a much larger reservoir of similar shape and fitted with a breathing hole to avoid pressure build-up in the oil circulation system. The system is shown here without insulation cladding.**

2.3.1 Synthesis of the PSU pre-polymer

The suppliers of chemicals are listed in Table 4. The PSU pre-polymer was synthesized reacting 145 g (0.64 mol) bisphenol A, 184.25 g (0.64 mol), 4,4'-chlorophenyl sulphone and 263.5 g (1.910 mol) K_2CO_3 in a 5 L reactor with 650 mL redistilled NMP and 312.5 mL redistilled toluene. A high-speed stirrer motor (Bonfiglioli Group, South Africa), attached to a stirrer blade was used to obtain thorough mixing at 230 RPM. The reaction was heated to 155°C using a heat-transfer oil (Thermia D, The Shell Company) recirculation system and maintained at that temperature for 4 h. During this period, a refluxing toluene/water azeotrope was formed from the reaction mixture and removed with the use of a Dean-Starke trap, while the temperature was raised to 190°C. Polymerization of the PSU pre-polymer was continued for 4 h at 190°C. The reactor was thoroughly flushed with N_2 gas before and after charging it with the reagents [6].

Table 4: PSU pre-polymer: list of chemicals used and suppliers

Materials	Grade	Supplier
bisphenol A	analar	Sigma-Aldrich, UK
4,4'-chlorophenyl sulphone		Sigma-Aldrich, Germany
potassium carbonate (K_2CO_3)		Merck Laboratory Supplies, RSA
Toluene		Protea Chemicals, RSA
N, methyl, 2-pyrrolidone (NMP)		BASF Corporation, Germany

2.3.2 Synthesis of the branched PEO prepolymer

The suppliers of chemicals are listed in Table 5. The branched PEO pre-polymer was synthesized using the equipment in Figure 6 by reacting 155.5 g (0.039 mol) 4 kDa dihydroxy-poly(ethylene glycol), 32.0 g (0.0195 mol), Tetronic 304 and 250.25 g (1.81 mol) K_2CO_3 in the 5 L reactor together with 437.5 mL redistilled NMP and 245 mL redistilled

toluene. A high-speed stirring motor (Bonfiglioli Group, South Africa) and dispersion stirrer was used for thorough mixing (230 RPM). The reaction was heated to 155°C using a heat-transfer oil (Thermia D, The Shell Company) recirculation system maintained at that temperature for 4 h. During this period a refluxing toluene/water azeotrope was formed from the reaction mixture, which was removed with the use of a Dean-Starke trap, while adding 11.75 g (0.046 mol) 4'4-fluorophenyl sulphone. The temperature was raised to 190°C. Polymerization of the PSU pre-polymer was continued for 6 h at 190°C. The reactor was thoroughly flushed with N_2 gas before and after charging it with the reagents.

Table 5: Branched PEO prepolymer: list of chemicals and suppliers Table 4

Materials	Grade	Supplier
dihydroxy-poly(ethylene glycol)		Merck Laboratory Supplies, RSA
Tetronic 304		BASF Corporation, USA
potassium carbonate (K_2CO_3)		Merck Laboratory Supplies, RSA
N, methyl, 2-pyrrolidone (NMP)		BASF Corporation, USA
toluene		Protea Chemicals, RSA
4'4-fluorophenyl sulphone		Sigma-Aldrich, Germany
methanol (MeOH)	HPLC	Fluka Chemie GmbH, Switzerland)

2.3.3 Synthesis of the branched PEO-block-PSU copolymer

Both reaction mixtures were allowed to cool down to 50˚C before the PEO pre-polymer was added to the PSU pre-polymer. This mixture was again reheated to 190°C and maintained at that temperature for 8 h while stirring (230 RPM). The equipment was purged with N_2 gas after the two pre-polymers were combined in the same reactor. The copolymer was then allowed to cool to room temperature, precipitated in demineralized water, neutralized with hydrochloric acid and washed thoroughly with demineralized water. The branched copolymer product was precipitated in water, recovered by filtration, and dried at 60˚C for at least 48 h.

2.3.4 Methanol extraction of branched PEO-block-PSU copolymer

Method 1

A solution of the branched PEO-block-PSU copolymer was prepared in NMP 30% (m/m). Methanol (MeOH) was added to this solution while stirring with magnetic stirrer bar equipment until the copolymer precipitates from the solution. The mixture was left until the two fractions were completely separated and the top layer, MeOH containing the extracted PEO fraction, was decanted. The lower fraction was placed in an oven at 60 ˚C for 12 h to evaporate the last remaining traces of MeOH. The remaining fraction was weighed and dissolved in NMP (30% m/m). This extraction of the copolymer was carried out three times before the copolymer was recovered for NMR analysis by precipitating it in deionised water.

Method 2

A 30% (m/m) solution of the branched PEO-block-PSU copolymer was prepared in NMP. MeOH was added drop-wise to this solution with a drip funnel over an extended period of time while stirring with a magnetic stirrer bar until the copolymer precipitated from the solution. A clear layer of excess MeOH was observed on top of the mixture. The top layer (MeOH containing the extracted PEO fraction) was decanted. The lower fraction was placed in an oven at 60 ˚C for 12 h until all remaining traces of MeOH had evaporated. The remaining fraction was weighed and dissolved in NMP (30% m/m). This extraction of the copolymer was carried out three times before the copolymer was recovered for NMR analysis by precipitation in deionised water.

2.4 Analytical techniques

The surface properties of the membranes experimented with as well as the properties and characteristics of the synthesized polymer additive were analyzed by means of a number of analytical techniques.

2.4.1 Dynamic contact angle determination

The dynamic contact angle (DCA) measurements were performed with a Cahn DCA Analyzer (Cahn Instruments, USA) and Cahn DCA Application Software, with distilled water as contact phase. Samples were used without prior drying to preserve the membrane structure and to minimize wicking. Three DCA measurements were made for each sample following stabilization. Average values and standard deviations were calculated from these values for each sample.

2.4.2 Atomic force microscopy

The determination of the membrane pore size was done in the contact mode with a silicon-tipped contact cantilever using either the atomic force microscope (AFM) Topometrix Explorer from Nanosensors (lower resolution) or the Multimode AFM from Veeco (higher resolution). Surface roughness was determined over an area of 25 μm^2 using the Topometrix AFM and over an area of 2 μm^2 with the Veeco AFM.

Digital pulsed force mode (DPFM)

Atomic force microscopy is based on the detection of atomic interaction forces between a sharp tip and the sample. A topographic image with (sub) nanometre resolution is generated by sampling the interaction force over a two-dimensional array. To prevent the interaction between the tip and the surface from destroying or modifying the sample, the interaction forces are often determined by force modulation techniques. In this intermittent contact, or tapping mode, the tip touches the surface only briefly during each cycle, and no lateral forces are present. Force spectroscopy can be performed by determining a force – distance curve [16] at a particular point on the sample. From this curve, physical properties, such as the adhesion or stiffness of the sample, can be determined.

The DPFM combines both techniques and generates a topographic image simultaneously with an image of, for example, the adhesion of the scanned area. The tip makes contact with the sample periodically and measures a force-distance curve at every point in the image. In this way a spatial map of the adhesion characteristics is determined.

In the digital pulsed force mode [17-20] the AFM is operated in contact mode with a sinusoidal modulation applied to its z-piezo. The modulation frequency is well below the resonance frequency (f_r) of the cantilever (force modulation cantilever with $f_r \approx 70kHz$) - in this case the modulation amplitude was set to 1kHz. In this way force-distance curves can be measured at every scan point, by continuously bringing the tip into contact with the surface and retracting it. Thus, topography and physical surface properties, such as stiffness or adhesion can be measured simultaneously and with the same spatial resolution.

The peak force shown in Figure 8b serves as the input for the control loop of the AFM to maintain a “constant” force mode. This force signal is used to obtain a topographical image of the sample. The adhesion force is determined by measuring the difference between the negative force peak and the baseline Figure 8c and is represented as an adhesion image of the sample. Each voltage value is allocated a colour value, which results in an adhesion image. Lighter colours represent higher adhesive forces.

To aid the interpretation of the results, each adhesion image was displayed as a histogram, as displayed in Figure 9. This shows the relative frequency with which each voltage value occurs within the scanned area. The average value represents the average adhesive force value, which corresponds to the average hydrophilicity of the sample. The standard deviation is a measure of the range of these values and serves as an error bar in our presentation of the data.

In the present study a silicon tip was used to scan the surface of the membranes. Untreated silicon has a native oxide layer with hydroxyl moiety. These OH groups are adsorption sites for water molecules and silicon with a natural oxide surface layer is therefore hydrophilic. A conventional silicon tip with SiO_2 groups at the surface will show a higher adhesive force with a hydrophilic than with a hydrophobic surface [17,19,20]. The image of the adhesion force therefore represents the hydrophilicity of the sample. Lighter parts represent more hydrophilic compounds and darker parts represent more hydrophobic compounds.
Quantitative values of the adhesive force F_{adh} are given by equation [24]:
$F_{adh} = V_{adh}CkS$

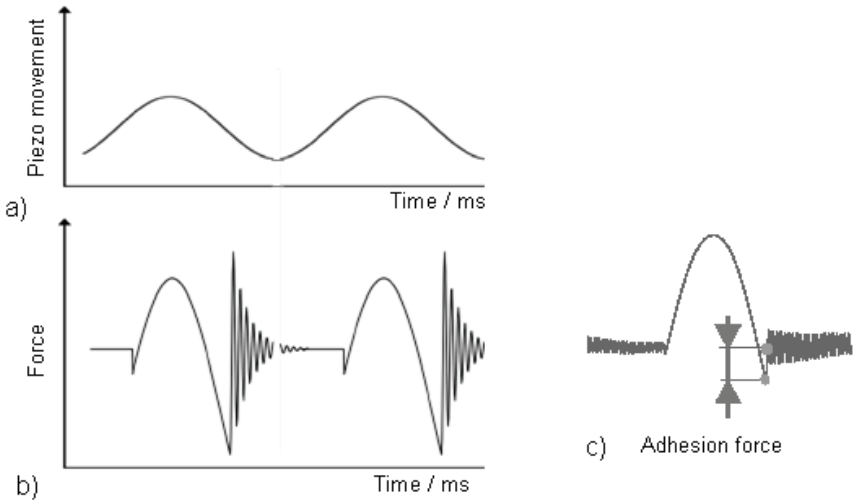

Figure 8: a) z modulation of the piezo, b) force signal as a function of time and c) adhesion force measured for each sinus cycle [21].

A similar technique was applied by Sato et al. [22] to determine the distribution of observed values of the adhesive forces on self-assembled sample surfaces. Okabe et al. [23] used this technique to discriminate the functional groups of self-assembled sample surfaces, by using chemically modified tips.

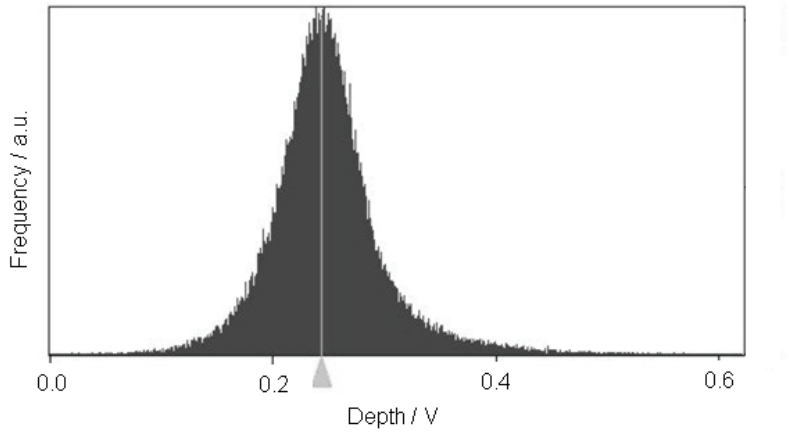

Figure 9: Histogram of the voltage distribution in an adhesion image.

Where V_{adh} is the average voltage value of the adhesion image, C is a machine dependant amplification factor (here $C = 1$), k is the spring constant of the cantilever and S the sensitivity of the photodiode. The spring constant k of the force modulation cantilever was 2.8 N/m [25] and the sensitivity S was determined to be 85.5 nm/V. The value of the spring constant was calculated from the dimensions given in the cantilever specifications. Although the actual spring constant might differ from this value, the resulting error is a constant scale factor that remains unchanged throughout all measurements. It therefore remains valid to compare the quantitative results of different adhesive force measurements.

All AFM measurements were made using a Veeco Multimode instrument with a Witec digital pulsed mode controller. Every image was recorded with a scan of 5 µm x 5 µm with a resolution of 256x256 pixels. The value of the adhesive force was therefore determined by averaging over 65 536 measurements. This presents a good statistic distribution, compared to the few individual force-distance measurements customarily used to describe adhesive forces. In later paragraphs we will demonstrate that the AFM in DPFM mode is a very useful and valid tool to determine the surface hydrophilicity of different membranes. Unlike other techniques it allows the reproducible determination of quantitative values with a statistical significance. The hydrophilicity of pure hydrophobic PSU membranes, and PSU membranes with 3 and 6 mass% hydrophilic contents in the casting solution were studied.

2.4.3 Scanning electron microscopy (LEO EDS-SEM procedure)

Wet membrane samples were cut, freeze-fractured in liquid nitrogen and allowed to dry out in the atmosphere. Imaging of the samples and analysis of the phase compositions were accomplished using a Leo® 1430VP scanning electron microscope (SEM) at Stellenbosch University. Prior to imaging or analysis the samples were sputter-coated with either gold or carbon depending on the application. Samples were identified with backscattered electron (BSE) and/or secondary electron imaging, and phase compositions quantified by EDS analysis using an Oxford Instruments® 133KeV detector and Oxford INCA software. Beam conditions during the quantitative analyses were 20 KV and approximately 1.5 nA, with a working distance of 13 mm and a specimen beam current of -3.92 nA. Despite the relatively low energy of the beam, X-ray counts with the set-up used were typically ~ 5 000 cps. The counting time was 50 s live-time. Natural mineral standards were used for standardization and verification of the analyses. Pure Co, as well as Ti and Fe in ilmenite were used periodically to correct for detector drift. Beam conditions during semi-quantitative analyses, when used in case of unpolished samples, were as described above without controlling the specimen beam current and the results were normalised to 100 mass%.

LEO SEM variable-pressure procedure
Variable pressure operation is a SEM mode where the vacuum-pressure in the chamber is higher than the vacuum in the column and gun. A fixed aperture is inserted between the chamber and the column and a different vacuum pump rate is applied to the chamber and column. The small number of gas particles in the chamber is ionized by the electrons expelled from the sample, which is then detected by the glass variable pressure detector. The beam conditions were an accelerating voltage of 25 kV and a spot size of 350, corresponding to approximately 1.5 nA. The working distance that gave the best results was 7 mm and the vacuum pressure in the chamber was set to 50 Pa at the start. Variable pressure operation is appropriate for samples that are damp, kept in alcohol or soft samples that will loose shape under high-vacuum conditions.

2.4.4 High-pressure liquid chromatography
The high performance liquid chromatography (HPLC) system used to determine molar mass of the synthesized products was the Waters 2690 separation module (Alliance) with an evaporative light scattering detector (ELSD) (PL-ELS 1000 from Polymer Laboratories Detector).

Control, data acquisition, and processing was provided by PSS Win GPC7 (Polymer Standards Service). The column set was 1PLgel 3 mm mixed-E 300*7.5mm (Polymer Laboratories) and the stationary phase was a highly cross-linked porous polystyrene/divinylbenzene matrix. The molar mass (M_w) of all samples was determined at 30°C at a flow rate of 1mL/min and tetra-hydro furan (THF) was used as the solvent. All M_w determinations are relative to polystyrene standards (EasiVial PS from Polymer Laboratories) used to calibrate the system.

2.4.5 Nuclear magnetic resonance
NMR spectra were recorded on either a 300 MHz Varian VXR spectrometer equipped with a Varian magnet (7.0 T)) operating at 300 MHz for ^{1}H and 75 MHz for ^{13}C; or a 600 MHz Varian Unity Inova spectrometer equipped with an Oxford magnet (14.09 T) operating at 600 MHz for ^{1}H and 150 MHz for ^{13}C. Standard pulse sequences were used to obtain ^{1}H, ^{13}C, and attached proton spectra (APT).

3.1.1 Extraction with methanol

MeOH is a selective solvent for PEO [8]. Effective extraction of the final product with MeOH will remove any PEO not covalently bound to the copolymer. If the extraction is carried out too quickly, the product will precipitate and ineffective extraction will result. The procedures are described in the experimental section and the results of each set of extractions are followed *via* NMR analysis (Figure 11). This analysis also allows the determination of the PEO content in the final product.

From the proton spectra (Figure 11) as well as the data presented in together with **the data regarding the molar mass of each sample obtained by HPLC.**

Table 7, one can notice the reduction in the PEO content of the copolymer sample following the first extraction procedure. After the second MeOH extraction a slight reduction is observed in the % PEO relative to the PPO content, while there is a slight increase in the % PEO relative to the PSU content. Following the third MeOH extraction the % PEO increases relative to the PPO content, while an increase occur in the % PEO relative to the PSU content. These results indicate that the PEO molecules, not covalently bound to PSU have been extracted and that further extraction with MeOH is unnecessary. The molar fraction of branch points also appears to stabilise following the extraction procedure. The increase in the molar mass of the samples after each extraction step, as well as the simultaneous reduction in polydispersity may be due to the fractionation of the branched copolymer during the aqueous precipitation following each MeOH extraction procedure. This was also observed by Hancock *et al.* [6].

The data obtained from these proton NMR spectra is presented in Table 8: Results of MeOH extraction using method 2 as described in the experimental section

Sample ID	**Molar fraction of branch points**	**% PEO relative to PPO**	**% PEO relative to PSU**
Copolymer prior to MeOH extraction	0.0103	92.27	61.83
Copolymer following 1st MeOH extraction	0.0141	89.78	47.44
Copolymer following 2nd MeOH extraction	0.0212	84.17	53.16

together with the data regarding the molar mass of each sample obtained by HPLC.

Table 7: Presentation of relevant information regarding the membrane modifying copolymer synthesized in the reactor system with the progression of the MeOH extraction as described in the experimental section (method 1).

Sample ID	**Molar fraction of branch points**	**% PEO relative to PPO**	**% PEO relative to PSU**	**Molar mass (Mw)**	**Polydispersity**
Copolymer prior to MeOH extraction	0.0103	92.27	61.83	42 568	3.11
Copolymer after 1st MeOH extraction	0.0126	91.16	53.22	43 191	2.96
Copolymer after 2nd MeOH extraction	0.0129	90.36	55.65	n/a	n/a
Copolymer after 3rd MeOH extraction	0.0126	91.53	50.37	47 367	2.06

The scaled-up reaction exhibited one draw-back when compared to the laboratory scale reaction. The product, synthesized with laboratory-scale equipment could be used for the preparation of membrane casting solution without additional cleaning procedures. In contrast, the product synthesized in the reactor system initially produced a hazy membrane casting solution. But, cleaning steps, including large-scale MeOH extraction or dissolving the product in NMP and precipitating it in water, improved the quality of the final synthesized product. Unfortunately, these processes are time consuming and lead to a loss of product. It is therefore important that the MeOH extraction procedure is optimized. A second method (method 2) was introduced and the results compared to those of the first method. The NMR results of this procedure are represented in Figure 12 and the data obtained from the relevant NMR analyses is presented in Table 8: Results of MeOH extraction using method 2 as described in the experimental section

Sample ID	**Molar fraction of branch points**	**% PEO relative to PPO**	**% PEO relative to PSU**
Copolymer prior to MeOH extraction	0.0103	92.27	61.83
Copolymer following 1st MeOH extraction	0.0141	89.78	47.44
Copolymer following 2nd MeOH extraction	0.0212	84.17	53.16

Table 8: Results of MeOH extraction using method 2 as described in the experimental section

Sample ID	Molar fraction of branch points	% PEO relative to PPO	% PEO relative to PSU
Copolymer prior to MeOH extraction	0.0103	92.27	61.83
Copolymer following 1st MeOH extraction	0.0141	89.78	47.44
Copolymer following 2nd MeOH extraction	0.0212	84.17	53.16

3.2 Membrane development

During the early phase of this project, membrane films were prepared by casting the membrane solutions on a glass plate followed by immersion into a non-solvent bath. These membrane test films were used to study the membrane surface characteristics, mainly with regard to the hydrophilic/hydrophobic nature of both modified and unmodified samples.

However, these membrane films are not ideal for the determination of flux and retention performances. Two additional membrane manufacturing techniques were used to produce flat-sheet as well as capillary membranes, using various casting solutions as described in the experimental section. Flux and retention information can be obtained from membranes produced by either of these two methods with the use of appropriate test equipment. Pore size determination of the different types of UF membranes is also possible with the use of AFM technology and the membrane morphology can be investigated using SEM photographs.

Membrane morphology plays an important role in the functioning and performance of a membrane. The membrane surface in contact with the solute often has a major influence on both membrane flux and retention characteristics. The porous substructure of the membrane merely acts as a support for the membrane skin layer. The substructure morphology should pose minimal resistance to mass transport as possible. Several factors that affect membrane morphology can be controlled during the phase inversion process.

The viscosity of the polymer casting solution significantly affects the porosity of asymmetric membrane produced by the phase inversion process. Casting liquid viscosities can be changed by increasing the membrane-polymer concentration in the membrane formulation [10] or by using additives such as polyvinylpyrrolidone (PVP) [11] or inorganic salts [12]. As the porosity of the membrane increases with an increase in the casting solution viscosity, pore size in the skin layer tends to decrease. The use of inorganic salts has been reported to suppress macro void formation [12]. The nature of the membrane surface layer can also be influenced by the non-solvent composition [13]. The pores in the surface layers of the UF membranes prepared for this study can only be measured by high resolution electron microscopy or AFM imaging. The use of AFM technology generally indicates larger pore diameters than those determined from SEM photographs. The AFM data is regarded as more accurate since membrane pore size and membrane structure may change due to the sample preparation methods used for SEM [14]. Both AFM and SEM techniques are used, in conjunction with flux and retention data, to determine the characteristics of flat-sheet and capillary membranes.

3.2.1 Flat-sheet membranes

Several membrane formulations were prepared to produce flat-sheet membranes. The formulations include membrane types #A, #B and #C that were successfully analysed for their increasing hydrophilicity by AFM (DPFM mode). These results, measured as the adhesive

force between the membrane and the AFM tip, are discussed later in the text, but are summarized in Table 9. Membrane types #A, #B and #C were prepared from similar casting solutions used for the test membrane films used during the AFM adhesion study. Poly(ethylene glycol) was added to these formulation used to improve the flux performance of the flat-sheet membranes (Table 1). Two additional formulations identified as types #Hand #Kwere also prepared and used for flat-sheet membrane manufacturing. These ultrafiltration membranes were tested regarding their PWF_{60} and PEG_{35K} retention characteristics. Pore size determinations were obtained using AFM technology and all results are presented in Table 9. Unfortunately the surface of the type #K membranes proved too rough for accurate pore size determination *via* AFM.

Table 9: Available information of the various flat-sheet membranes

Membrane Identification	Membrane modifying copolymer added (% m/m)	Adhesive forces - AFM determined (nN)	PWF (L/m^2h)	Pore size (nm)	PEG_{35K} retention (%)
Type #A	0	60	152.8	70.8 (± 14.3)	18.5
Type #B	3	120	130.3	77.6 (± 13.4)	47.8
Type #C	6	175	69.5	22.0 (± 2.48)	96.8
Type #H	0	N/D	151.2	61.7 (± 9.8)	97.1
Type #K	12	N/D	173.0	N/D	22.9

Pure water flux (PWF)
Not determined (N/D)
Note: Membrane types marked with an asterisk were dense films, without PEO addition, used for analytical purposes

For membrane types #A, #B and #C the PWF_{60} data decrease with an increase in the total polymer content. The pore sizes obtained for membrane types #A and #B appear to be quite similar, but there is quite a difference between the pore sizes of the #A and #C type membranes. The discrepancy between the type #B membrane's pore size and PEG_{35K} retention data may be explained by the fact that surface roughness affects the AFM accuracy. PEG_{35K} retention data clearly show the correlation between the increase in the membrane's retention of the PEG_{35K} molecules due to a decrease in pore size and the increase in the polymer content in the membrane's formulation.

When compared to each other, the type #H and type #K membranes also exhibit different PWF_{60} data as well as large differences in retention of PEG_{35K}. It is clear that the substitution of 12% (m/m) of the PSU in the type #H formulation with 12% (m/m) of the membrane modifying copolymer in the type #K formulation, affected the permeability of the respective membranes. Both flux and retention data in Table 9 suggest that the type #K membrane has larger pores than the type #H membrane. The casting solution of the type #H membrane is the more viscous of the two casting solutions. This difference in viscosity almost certainly plays a role in the different characteristics obtained for the resulting membranes. Unfortunately, the viscosity of these membrane formulations is too high to allow accurate determination by the available equipment. The data in Table 9 supports previously published results [12] stating that the membrane pore size in the skin layer decreases as the viscosity of the membrane casting solution increases.

During membrane testing with the PEG_{35K} solution, flux data was obtained for these membranes after one hour. The type #H membrane's flux was reduced by 65.14% while the type #K membrane's flux was reduced by only 35.25% compared to the PWF_{60} determined for these membranes. Membranes were then flushed with pure water for one hour and the resulting PWF for the type #H membrane improved to 73.12% of the initial flux (PWF_{60}) while the PWF for the type #K membrane recovered to 95.93% of the original PWF_{60}.

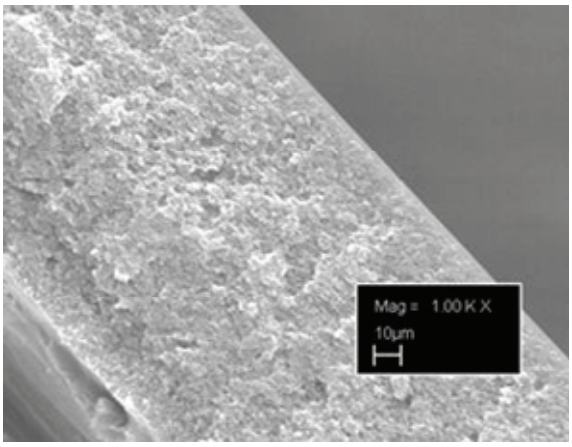

Type #H air dried
low magnification

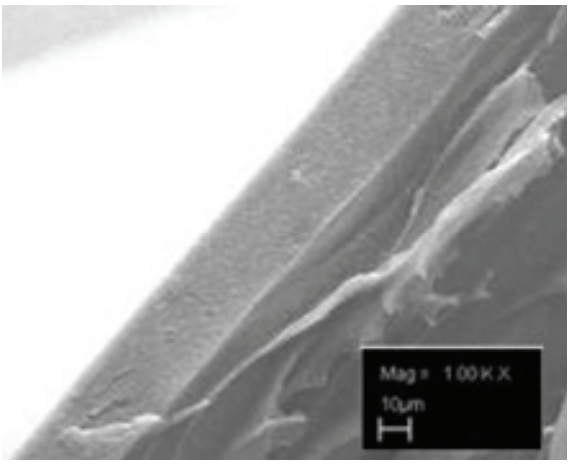

Type #K air dried
low magnification

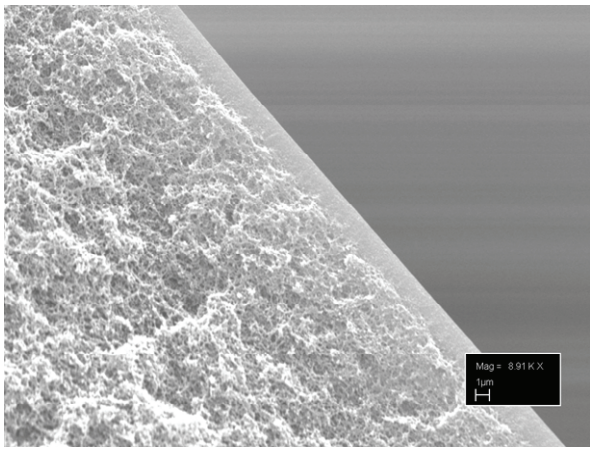

Type #H air dried
high magnification

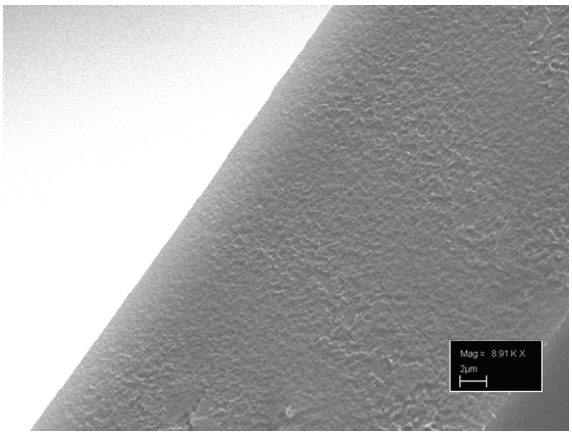

Type #K air dried
high magnification

Figure 13: SEM pictures showing the flat-sheet membrane morphology of the type #H membrane on the left and type #K on the right at different magnification.

The SEM images presented in Figure 13 may provide some answers to the different flux- and retention characteristics of the two membrane types. The type #H membrane exhibits the thin, dense skin layer and porous membrane morphology typical of asymmetric membranes. The type #K membrane's outer skin layer is less well defined than that of the type #Hmembrane. The morphology of the type #K membrane appears to be more sponge-like and gradually changes in density from the top layer to a less dense morphology for the lower layers. The differences exhibited by the respective skin layers of the two different types of membrane were expected due to the changes in the respective membrane solutions. These changes are also expected to influence the flux and retention performance of the different membrane types. Actual PWF data as well as PEG_{35K} retention determinations obtained for

type #H and #Type K membranes (Table 6) reflects these changes in membrane performance due to the addition of the membrane modifying copolymer. These findings were in correspondence with literature [10,15].

3.2.2 Capillary membranes

Although UF membranes are used in a number of different industrial and water purification applications, the protein purification industry in particular, can benefit from advances in membrane separation technology. Large-scale protein purification is expensive and in this competitive industry where membrane separation is an integral component of production costs and product quality, membrane technology can make the difference between success and complete failure. Further, proteins are known to cause membranes to foul. It was for this reason that enzyme separation was incorporated into the study, making use of a well-defined biological feed stock solution that was consistent in its character to ensure repetitive membrane performance results.

The enzyme chosen as candidate foulant in this study was horseradish peroxidase (HRP). The purified enzymes are used in applications varying from laboratory applications to large scale digestion of waste in the paper manufacturing industry.

A number of capillary membrane formulations similar to type #P but with small variations (Table 10) were prepared and used in the production of capillary membranes. The most promising of these capillary UF membranes were types #P, #L and #M. UF membrane type #P shows high retention of horseradish peroxidase (HRP) as well as high flux. These characteristics make the type #P an excellent membrane for the separation of stock solutions containing HRP. The type #L membrane shows even better retention of the HRP enzyme and can be considered for use in membrane diafiltration applications.

Diafiltration is one technique for the removal of the salt used to precipitate proteins from a solution. The volume of the feed in these applications is small compared to the bulk solutions from which the protein is purified. In order to minimize protein losses during the process of diafiltration, the protein retention characteristics are a greater priority than high water flux throughput. For this reason, although the type #L membrane shows a much lower PWF_{60} than the type #P, its higher HRP retention makes this membrane an excellent candidate for use as a diafiltration membrane. Both the type #P and #L membranes have immediate applications in the protein purification industry and both can be modified successfully by incorporating the branched PEO-block-PSU copolymer into their respective membrane formulations to yield membranes with a more hydrophilic character. Both type #M and #N membranes show excellent HRP retention characteristics. Further efforts to develop a membrane that combines a very high (> 99%) HRP retention with high flux will apply the knowledge gained from developing these prototype membranes.

Even though some success have been achieved regarding the manufacturing of the type #P and type #L UF capillary membranes, the development work regarding these membranes are far from complete. This development work include the suppression of macro-void formation (Figure 15) as well as increasing the membrane flux and obtaining better control regarding the retention characteristics of these membranes. Macro-voids are present in the substructure of the capillary UF membranes manufactured during this study (Figure 15) and may present problems regarding membrane flux as well as structural integrity of these membranes [10].
Additional research will be performed to suppress macro-void formation without sacrificing high flux or retention characteristics of the existing type #P membrane. These improvements, as well as hydrophilizing these membranes are under way. Despite the obvious advantages

inherent in hydrophilizing these UF membranes, the effect of this modification on the membranes' effectiveness in the protein purification industry may not be beneficial in all applications. The different iso-electric points of proteins, as well as the pH and ionic strength of various feed solutions will have to be studied carefully to ensure that the hydrophilic membranes are used only where they can be of real benefit. Such applications may be oil-water separation or for the treatment of surface water containing humates, to mention two.

Table 10: Flux, HRP and PEG_{35K} retention characteristics of capillary membranes

Membrane type	PWF_{60} (L/m^2.h)	HRP Retenion (%)
Type #D	379.7	85.7
Type #P	309.9	97.7
Type #J	104.6	94.2
Type #L	167.0	98.9
Type #M	160.9	98.9
Type #N	147.8	99.4

Unfortunately, the subsurface morphology of membranes cast as flat-sheets or test films show little resemblance of the morphology and character of capillary membranes manufactured from the same formulations. It is not too difficult to argue why. Membranes shrink during the phase inversion (Figure 14) and precipitation processes by up to 14% from their original wet, nascent, state.

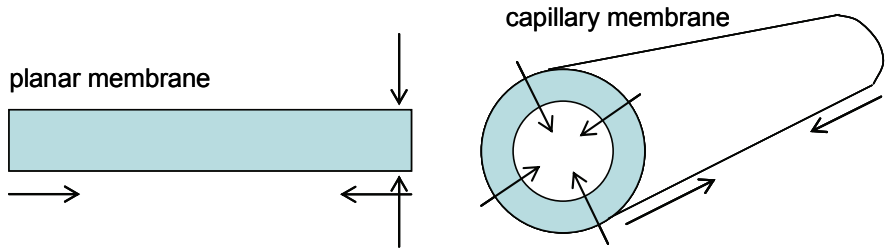

Figure 14: Shrinking direction of flat-sheet and capillary membranes during fabrication.

As can be seen from Figure 14, planar membranes shrink in two dimensions, as indicated by the arrows. This is not the case with capillary membranes that rather shrink in three dimensions. In the case of capillary membranes, the conformation and energy state of macromolecules in the nascent membrane is affected. This causes localized energy perturbations and possibly nucleation of solvent-rich sites. Ingress of bore-side coagulant into the nascent membrane substructure through micro-fissures that develop because of stress relief in the internal skin cause a rapid growth of these nucleation sites as the surrounding polymer bulk shrinks away and solvent from the bulk diffuses into these rapidly growing macro voids. This is not the case with flat-sheet membranes, as the skin layer does not endure the same amount of stress as that of the capillary membranes.

The problem is not insurmountable, though. By careful formulation, the spinning solution can be modified to favour spinodal decomposition rather than nucleation and growth of the respective phases. As a start, a formulation can be generated that is situated very close to the binodal on the ternary phase diagram, which will tend to favour spinodal decomposition and the formation of a lacy substructure.

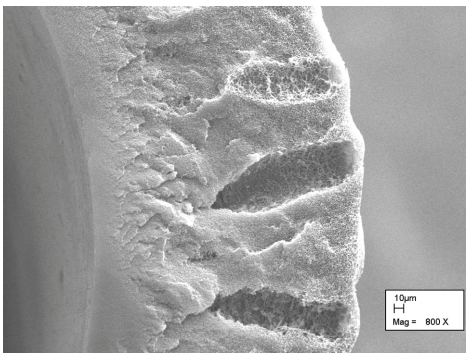

Type #D capillary UF membrane

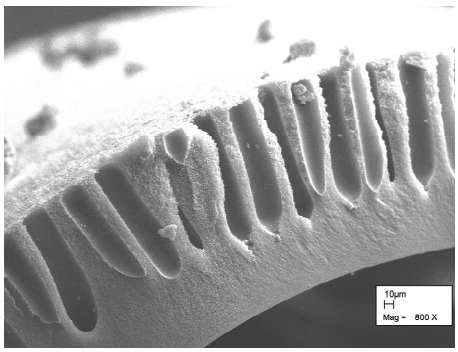

Type #P

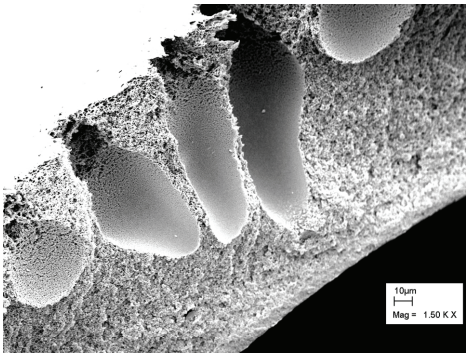

Type #J

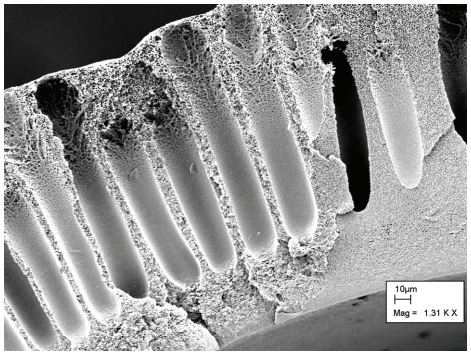

Type #L

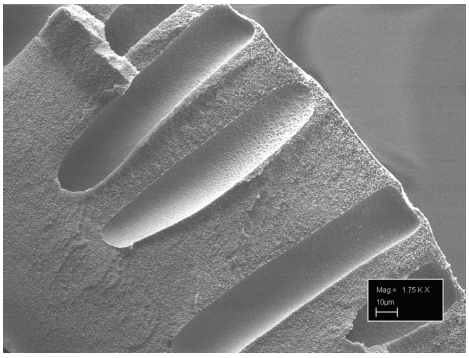

Type #M

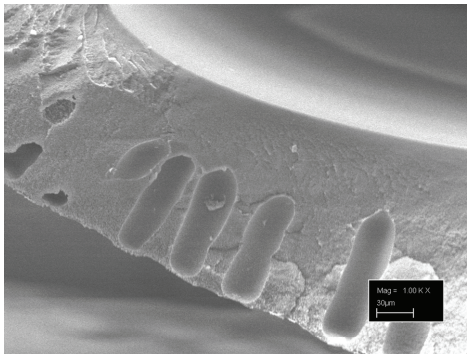

Type #N

Figure 15: SEM images of the different membranes characterised in Table 10. These different membranes all show macro-void formation, that may have to be suppressed in order to improve the mechanical quality of the membrane.

The aim of this project was to produce hydrophilic modified membranes with high product flux and acceptable retention of specific solutes. Only membrane types conforming to these criteria were tested in full scale operating systems.

3.3 Hydrophilization of polysulphone ultrafiltration membranes

One advantage of this membrane modification method is the homogenous modification of both internal and external membrane surfaces during phase inversion. Membrane modification is achieved by simply blending the branched PEO-block-PSU copolymer into the membrane-forming solution. This eliminates the costly and elaborate post-treatment hydrophilization processes previously mentioned. The covalent linkage between the hydrophilic-branched PEO block and the hydrophobic PSU block allows the preservation of the membrane surface integrity during use. It also helps to avoid problems associated with slowly desorbing adsorbates [1,5] and resultant loss of initial hydrophilization. This membrane modification technique, using the amphiphilic copolymer, can be applied to any membrane dependent process where lower hydrophobicity of the membrane surface is

required to reduce fouling. This is especially true for UF and MF membranes, where the preferred material of construction is hydrophobic.

The cost-effective manufacturing of modified PSU membranes, according to the method developed by Hancock *et al.* [1] will require a thorough understanding of the factors influencing the optimal molecular rearrangement of the amphiphilic copolymer at the membrane surface during the phase-inversion membrane manufacturing process.

It is important for future membrane development and manufacturing to determine the effect of adding various amounts of the branched membrane modifying copolymer to membrane formulations and to study its effect on the hydrophilic character of the modified membrane samples. The addition of an amphiphilic copolymer to a non-aqueous solution like the membrane casting liquid described in the experimental section will change the physical characteristics of the casting liquid. Changes in the nature of the casting liquid may be crucial to the preparation of viable UF membranes. As these changes may be just as significant to future development of the modified membranes as the hydrophilic surface modification itself, the effect of the addition of the membrane modifying copolymer on the flux and permeability of the resulting membranes were investigated as well.

In order to detect an increase in the hydrophilic character of the modified membranes, dynamic contact angle (DCA) and energy dispersive spectrometry (EDS) analyses techniques were used. These results were compared to additional analytical work with the use of a new AFM method, which combines conventional topography imaging with adhesive force mapping on the investigated surface. Porous and uneven membrane surfaces do not provide ideal surfaces for analysis via contact angle determination. AFM adhesive-force determinations were obtained to indicate changes in the hydrophobic/hydrophilic nature of the modified membrane surfaces. The AFM results should complement the results obtained using more conventional techniques and has the added advantage that these results should not be affected by surface roughness or porosity.

This method allows the quantification of the changes in the hydrophobic/hydrophilic character of modified PSU membranes.

3.3.1 Dynamic contact angle measurements

Contact angle measurement provides an indication of the degree to which a liquid will wet a particular surface. Similar surface energy for both liquid and the surface under investigation will mean that a droplet of the liquid will spread easily over a wider area of the surface, reducing the contact angle between the liquid droplet and the flat surface. Increasing differences between the surface energies of both the liquid and the solid surface will lead to increasing contact angles between the droplet and the solid surface. When water is used as the liquid (high surface energy), low contact angles will be measured between a water droplet and a polar surface (high surface energy), while high contact angles will result when analysing a non-polar surface (low surface energy). When attempting to decrease the contact angle between water and a particular solid surface, the polar content of the solid surface must be increased. This can be done, for instance, by adding hydroxyl groups to that particular surface. This will increase the surface energy of the solid surface and render it more hydrophilic.

The advancing contact angles [26,27] determined for the modified membrane surfaces (types #B*, #C* & #D*) prior to annealing, as displayed in Figure 16, are significantly lower than the advancing contact angle obtained for the similarly treated, unmodified membrane sample

of type #A*. This reduction in the advancing contact angle indicates an increased surface polarity and therefore a reduced hydrophobic character of the modified membranes [27,29]. The data presented in Figure 16 indicates that this reduction in the hydrophobic character of the different membrane samples, prior to annealing, is the result of increasing the amount of the branched PEO-block-PSU copolymer added to the membrane formulation.

Hancock *et al.* [1] published data of modified PSU membranes where the advancing contact angles were reduced by as much as 20 degrees compared to the 8 degree difference achieved in our experiments. However, direct comparison between the two sets of data would not be constructive. The data published by Hancock *et al.* refers to work done with linear PEO-b-PSU di-block copolymers without the branched copolymer architecture. That work was also concerned with the investigation of microporous membrane surfaces of which both the membrane preparation, relative amounts of the membrane modifying copolymer and surface topology are completely different from the ultrafiltration-type membrane surfaces that were the target of our investigations. However, the published data also showed that by increasing the membrane modifying copolymer added to the membrane formulations, the membrane modifying effect could be increased.

The effect that annealing has on the advancing contact angles of the different membrane series is displayed in Figure 16. Annealing initially appears to increase the advancing contact angles for all the membrane series, except for series #C. A reduction in the advancing contact angles for the different membrane series occurs only for annealing times larger than 10 to 15 h. The advancing contact angles for the unmodified membrane series (series #A) exhibit this same general tendency.

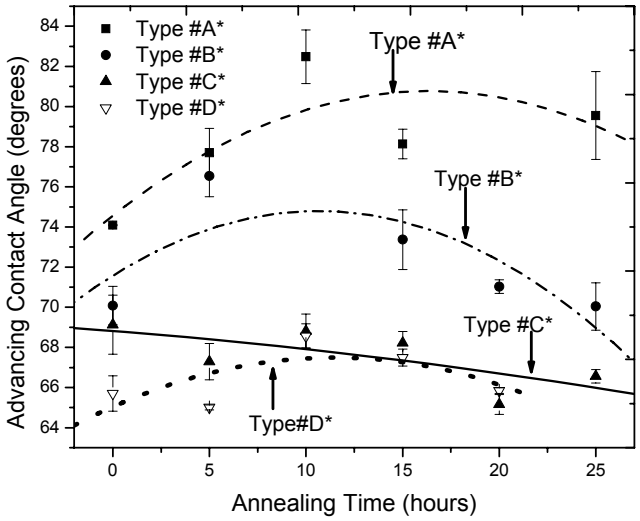

Figure 16: Advancing contact angles for the flat-sheet membrane types #A*, #B*, #C* and #D* at different annealing times.

To our knowledge, this is the first observation regarding the influence of different annealing times of the PSU membrane surface, independent of any additional modification of the chemical structure of the membrane. Annealing, even over a period of 25 h period failed to decrease the contact angles for membrane types #A*, #B* or #D* compared to their initial contact angles. The total reduction of only two degrees in the advancing contact angle for types #C* with annealing is rather small compared to the difference of 8 degrees between the advancing contact angles of types #A* and #D*, prior to annealing. Annealing, as described, clearly does not offer any additional advantages with regard to membrane hydrophilization.

For the modified membrane with the 6% hydrophilic content (type #C*), on the other hand, the contact angle decreased almost linearly with increasing annealing time.

3.3.1.1 Summary

The membrane surface-modifying branched block copolymer added to the membrane casting liquid significantly reduced the hydrophobic character normally associated with PSU membranes as indicated by the reduction in contact angles (Figure 16). Decreasing contact angles for the various modified surfaces is an indication that the surfaces became more hydrophilic (more polar with progressive higher surface energy) as larger amounts of the modifying copolymer were added to the membrane casting formulations.

3.3.2 Energy dispersive spectrometry

Advancing contact angle data indicates that membrane modification increases the surface polarity of the membranes. This modification process included the addition of increasing amounts of the branched PEO-block-PSU copolymer to the membrane casting solution as described above. During the phase inversion membrane preparation method, the PEO segments of the branched PEO-block-PSU copolymer arrange at the membrane surface [5]. Successfully modified membrane surfaces should therefore contain more oxygen than sulphur, compared to unmodified membranes. Energy dispersive spectrometry (EDS) analysis was used to determine the relative mass percentage change between the oxygen and sulphur content at the surfaces of the different membrane samples. Unlike DCA analysis, the EDS technique allows independent analyses of either the upper or bottom surfaces of flat-sheet membrane samples. This advantage of the EDS analysis technique over DCA measurements is important since the membrane preparation technique of phase inversion is dependent on liquid-liquid phase separation mechanisms [29,30], especially when using an amorphous polymer like PSU. Membrane preparation *via* phase inversion is expected to yield a membrane with two different types of surface, as displayed in Figure 17, identified for the purposes of this study as type α-and β-surfaces.

The surface of the cast membrane solution (type α) is in initial contact with the non-solvent coagulant during the phase inversion process while the other surface (type β) is in contact with the glass casting plate. Non-solvent diffusion will occur from the direction of the α-surface towards the β-surface. Membrane precipitation can be expected to occur almost instantaneously at the α-surface. This surface layer gels, to form a dense, skin-like interface between the coagulant and the nascent membrane-forming polymer solution [30,31] not yet in contact with the non-solvent (Figure 17). Using pure water as non-solvent, the fast rate of coagulant diffusion will lead to spinodal decomposition of the nascent membrane-forming polymer solution. Liquid-liquid separation of the two phases will occur and separate into interconnected regions of high and low polymer concentrations [1,30]. This intertwined network of phases will result in polymer-rich and polymer-poor phases that will solidify with the replacement of the solvent by the non-solvent, resulting in the precipitation of the membrane structure. The polymer-rich phases will tend to be more hydrophobic, consisting of PSU as well as the branched PEO-block-PSU copolymer molecules. The membrane modifying copolymer molecules will tend to arrange with the more hydrophilic PEO blocks associated with the more hydrophilic polymer-poor phase while the PSU blocks of this copolymer are expected to remain firmly embedded in the polymer-rich phase. As membrane precipitation occurs in the direction of diffusion of the non-solvent, the resulting membrane will exhibit two different types of surface, probably modified to different degrees by the branched, block copolymer.

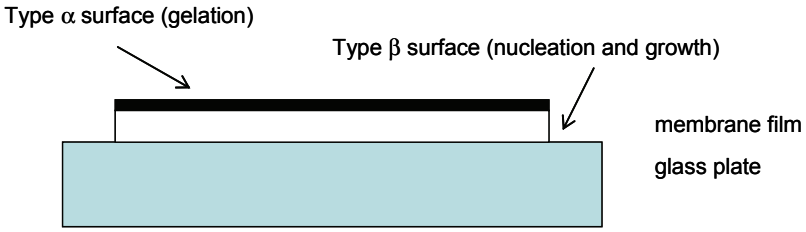

Figure 17: Schematic diagram of the α-and β-surface layers of a membrane.

Figure 18a shows the correlation between the amount of branched PEO-block-PSU copolymer added to the membrane formulation and the degree of oxygen (PEO) enrichment at the β-surface. As the amount of copolymer in the membrane formulation is increased the degree of surface oxygen enrichment at the β-surface increases as well. Theoretically the amphiphilic copolymer should have more time to arrange optimally at the polymer-rich/polymer-poor interface during spinodal decomposition. However, this oxygen enrichment is not linear, proving that membrane precipitation at this surface (β) still occurs before the full complement of the additional copolymer can arrange at the membrane surface. Similar results obtained for the α-surface (Figure 18b) show an increase in the oxygen content (PEO) of the membrane surfaces with increasing amount of modifying copolymer. However, the oxygen content of the modified α-surfaces does not change significantly with the increase in the amount of branched PEO-block-PSU copolymer added to the membrane formulation. Furthermore, the total oxygen content (mass percentage) at the α-surface of type #D* (with the highest amount of copolymer) is slightly less than at the β-surface. This pattern of oxygen enrichment suggests that the precipitation rate of the membrane polymer solution is important for an optimum PEO migration and therefore surface modification. The EDS technique was also used to investigate the effect of annealing on the arrangement of the PEO segments at the β-surface of the membrane. The results in Figure 18 show the effect of annealing on the β-surface oxygen content of membrane samples #A* and #D*. Annealing increases the surface oxygen content at the β-surface of both the modified (#D*) and unmodified (#A*) membrane series although the oxygen content at the β-surface of membrane series #D* remain significantly higher.

This increase in the oxygen content observed for these membrane samples (Figure 19), including the unmodified type A*, appeared to depend on annealing rather than the addition of the branched PEO-block-PSU copolymer. The most likely explanation for this phenomenon is the increased mobility of the unmodified PSU polymer molecules during the annealing procedure. The hydroxyl terminal ends of these molecules, when at the membrane/water interface will be in an optimum location to undergo hydrogen bonding or polar interactions with the polar annealing medium (water). Further, non-polar interaction between the benzene rings of similarly aligned PSU polymer molecules could then contribute to lock these molecules in place, conferring a small degree of crystallinity to this normally amorphous polymer. During annealing in water conditions will definitely favour such a concentration of mobile hydrophilic or polar groups at the membrane/water interface. The terminal groups available for such actions represent a very low proportion of the surface groups compared to the bulk polymer or copolymer at the surface but such a polymer rearrangement during annealing adequately explains the small but consistent increase in surface oxygen enrichment of both modified and control polymer films.

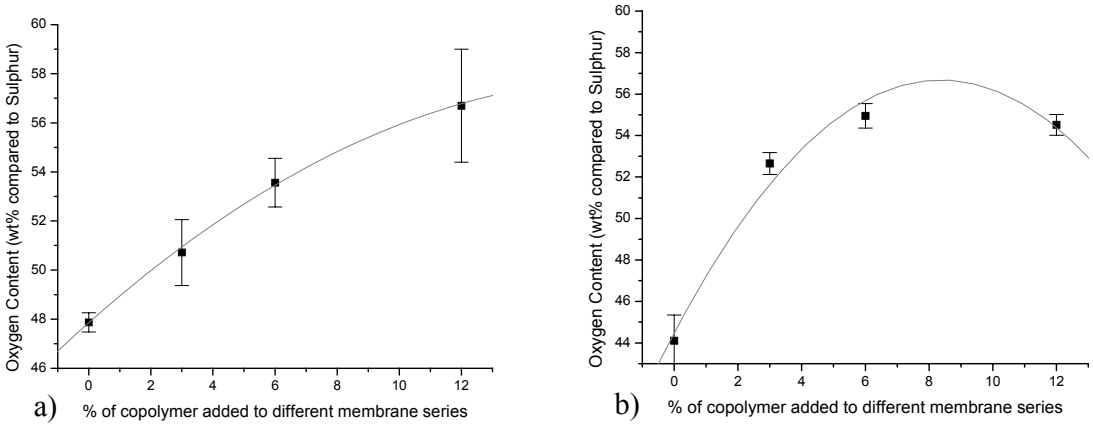

Figure 18: Oxygen as a mass percentage of the combined oxygen and sulphur content of the PSU membrane surfaces prior to annealing. a) β-surface, b) α-surface.

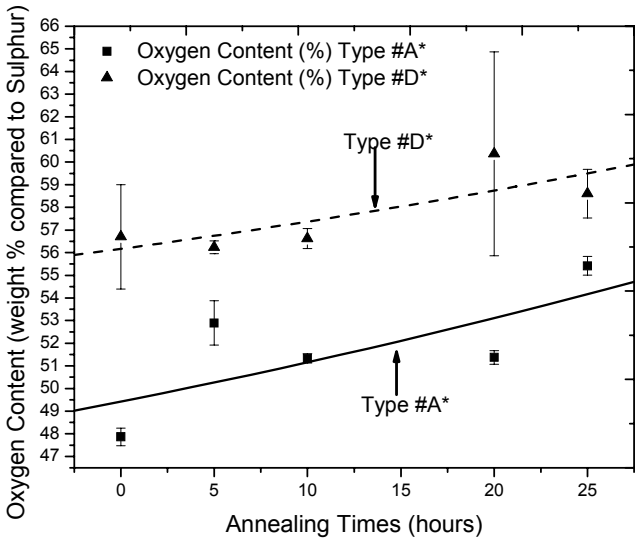

Figure 19: EDS results of the respective β-surface of types #A* (unmodified) and #D* (modified) membranes. The oxygen content measured for both these surfaces increased slightly with annealing over time.

3.3.2.1 Summary

EDS data confirmed that the increase in membrane polarity was a result of oxygen enrichment of the modified membrane surfaces. These results were consistent with the expectation that the PEO segments of the branched PEO-block-PSU copolymer arranged at the membrane surface during phase inversion. The analysis of both the α-and β-surface of the membranes by EDS indicated that the conditions during the membrane precipitation process affect the degree of molecular rearrangement of the PEO segments at the precipitating membrane/non-solvent interface and could hold the key to optimization and control of membrane hydrophilization. The effect of annealing may require additional investigation as it appeared to influence the membrane surface of both modified and unmodified membranes.

3.3.3 DPFM-AFM measurements

Figure 20 and Figure 21 show examples of the topographic and the adhesion images acquired for two different membranes. Figure 20 shows the surface of pure hydrophilic PSU. Although the topographic image shows large structures with significant height differences, which are probably PSU crystals, the adhesion image of the same area is almost uniform.

This indicates clearly that the topography does not influence the adhesion characteristics of the sample. Colour differences in the adhesion image are therefore due to differences in adhesive force, independent from topography.

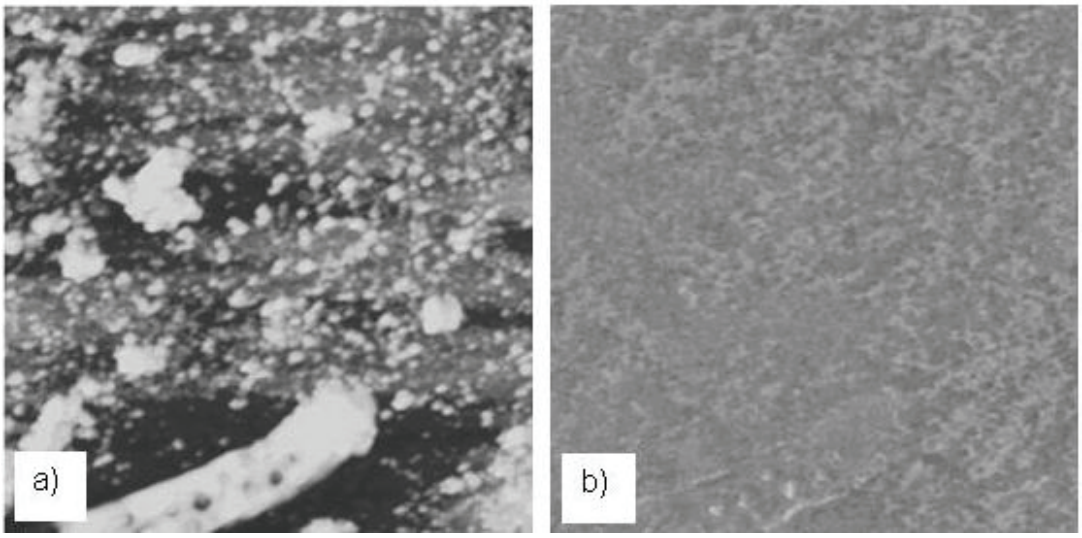

Figure 20: Pure PSU, scan size 5 μm x 5 μm. a) topography, b) adhesion.

Figure 21 shows the images of a hydrophobic PSU membrane with 3% hydrophilic content (PEO-block-PSU copolymer). Although the topographic structures in Figure 21a are less pronounced than in Figure 20a, the differences in adhesive forces in Figure 21b are visible. The surface is more hydrophilic, as represented by the lighter colour with few hydrophobic structures (dark areas). These could be PSU crystals, which have segregated to the surface. The segregation of particles of the same size was also confirmed by scanning electron microscopy studies. (Cyclic PSU polymers of low molar mass are known to form during PSU synthesis. They are far less soluble in the strong solvent that is used in the formulation than the mother material and tend to precipitate first. These particles seem to migrate towards the polymer-poor phase and are expelled from the membrane structure. They appear as the darker spots in Figure 21b, indicating little adhesion and therefore no hydrophilicity.)

Images such as Figure 20 and Figure 21 were acquired for control PSU membranes and membranes with 3% and 6% hydrophilic contents. For all three membrane types the annealing times ranged from 0 to 25 h.

The main problem of the experimental setup was the absence of an environmental chamber, which means that measurements performed on different days, under possibly different humidity conditions might not be comparable in their absolute values. However, all measurements were performed in an air-conditioned room at constant temperature. The different membrane series were measured within 1 to 2 h under the same conditions, so that the absolute values within one curve are statistically significant. An attempt was made to normalise the y-position of the curves for the different sample series by measuring the adhesive force of a standard sample before investigating the membrane series.

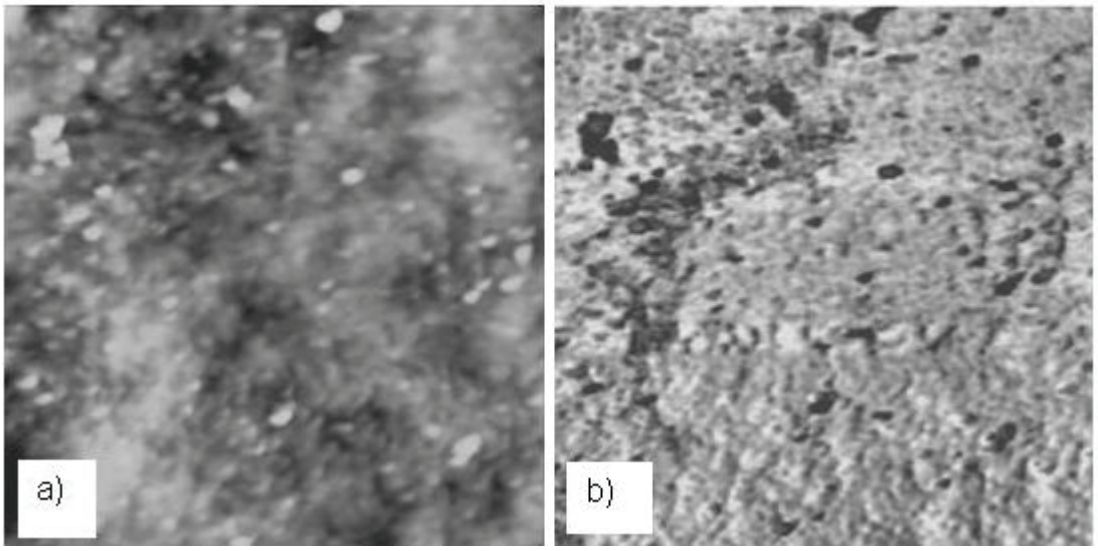

Figure 21: PSU with 3% hydrophilic contents, scan size 3.5 µm x 3.5 µm: a) topography, b) adhesion.

Each image resulted in an average adhesive force and a standard deviation, which describes the distribution of the adhesive force in the scanned area.

Figure 22 show that the annealing time has little influence on the hydrophilicity of the PSU membranes (■). The adhesive force increases only about 10nN, to a maximum value of 70nN ± 10nN after annealing for 20 h. In contrast, type #B* membranes, with 3% hydrophilic contents (●), show greater adhesive forces and a larger distribution of values. Even without any annealing the adhesive force is about 115nN ± 20nN. This indicates that the surface of those membranes is more hydrophilic than the surface of the pure PSU membranes. It can also be seen that the annealing time influences the surface hydrophilicity and its distribution. The adhesive force increases to a maximum value of about 170nN ± 40nN for an annealing time of 20 h. After this maximum value the value of the adhesive force decreases again – an increase in annealing time no longer results in a more hydrophilic membrane surface.

The larger distribution of the values of the adhesive force can be explained by the surface segregation of hydrophobic PSU crystals, as displayed in Figure 21. As the surface becomes more hydrophilic, as indicated by the lighter colours, there are also more hydrophobic particles, which results in a wider distribution of values.

For the membrane type #C*, with a hydrophilic content of 6%, the effect is even more pronounced. The adhesive force measured on the un-annealed sample is around 170nN with a wide distribution of ± 50nN. Again, this can be explained by the surface segregation of hydrophilic particles, which leads to a larger distribution of values. The adhesive force increases with increasing annealing time to about 220nN ± 60nN. No maximum value and subsequent decrease in the adhesive force was found for this membrane series and annealing of more than 25 h may have to be investigated.

The adhesive forces measured between the α-surface of the membranes and the hydrophilic silicon tip of the AFM (Figure 22) are significantly lower for the unmodified PSU membrane surface (60 nN) than for the modified PSU membrane surfaces of types #B* (120 nN) and #C* (175 nN). Type #D* could not be analysed with this method, since the attractive forces were too strong and the AFM cantilever stuck to the sample surface.

The adhesive forces displayed in Figure 22 show a similar pattern to the EDS results (Figure 22b) for the α-surface of the same samples. These results showed that the addition of the membrane modifying copolymer makes the membrane surface more hydrophilic, whereas the effect of annealing was relatively small and probably due to changes in the membrane topography.

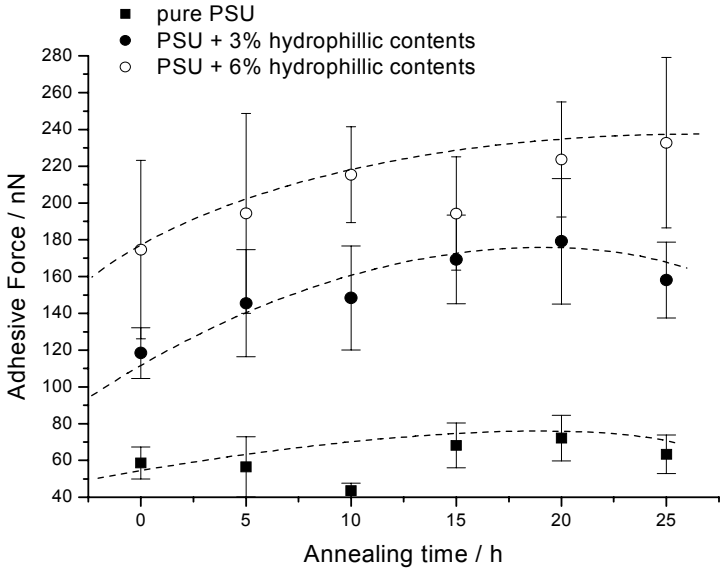

Figure 22: Hydrophilicity of the different membranes as a function of annealing time measured by DPFM.

3.3.3.1 Summary

DPFM-AFM measurements provided a very sensitive method for the determination of the hydrophobic/hydrophilic character of the modified membrane surfaces. This technique confirmed the data obtained from contact angle determinations and EDS analyses indicating hydrophilization of membrane surfaces by incorporating the membrane modifying copolymer in the respective membrane casting liquids. The results obtained for this study indicated that AFM pulsed force measurements may become a powerful tool for future studies regarding membrane surface modifications.

3.3.4 Flux and retention measurements

To investigate flux and retention characteristics of the modified membranes, 20% (m/m) PEG_{200} were added to the membrane films of types #A*, #B* and #C* to prepare types #A, #B and #C membranes. PEG is known to enhance the pore formation during the phase inversion of UF membranes [19]. The average pore size was determined from different AFM topography images similar to those presented in Figure 23. The membranes were not annealed and their respective flux (PWF_{60}) and PEG_{35K} data are presented in Table 4.

It can be noted that the PWF_{60} decreases with an increase of the modifying copolymer content, or with increasing surface hydrophilicity. The PEG_{35K} retention results (Table 6) show clearly the correlation between the increase in the modifying copolymer content and the increase in the respective membrane's retention of the PEG_{35K} molecules due to a decrease in pore size (Table 10).

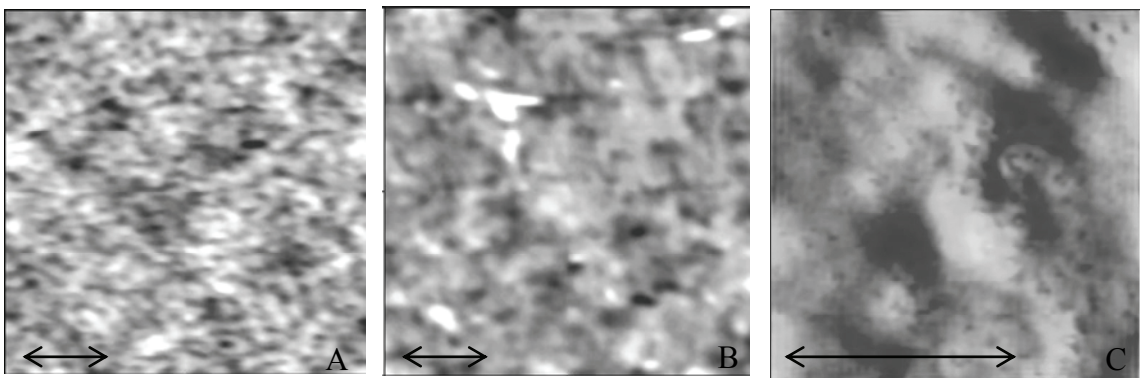

Figure 23: Topography images with pores of membrane types #A, #B and #C. The bar size is 500nm.

These results are not unexpected, since an increase in the polymer fraction of the membrane casting formulation has been reported to decrease the pore size while increasing the porosity [20].

3.3.5 Fouling experiments

A solution containing the HRP enzyme was concentrated using the Type #H ultrafiltration membrane. This solution was filtered through a 5 μm cartridge filter before membrane filtration to remove larger particles. The reject stream was returned to the feed solution while permeate was removed to concentrate the feed solution. Due to the rapid loss of flux over the duration of each concentration cycle (Figure 24 and Figure 25), a chemical cleaning procedure using a NaOH-and a sodium hypochlorite solution was followed to restore the membrane flux after each cycle. PWF data was determined after each step of the procedure to study the fouling effects of the HRP solution as well as the flux restoration effects of the chemicals (Figure 23) on membrane performance.

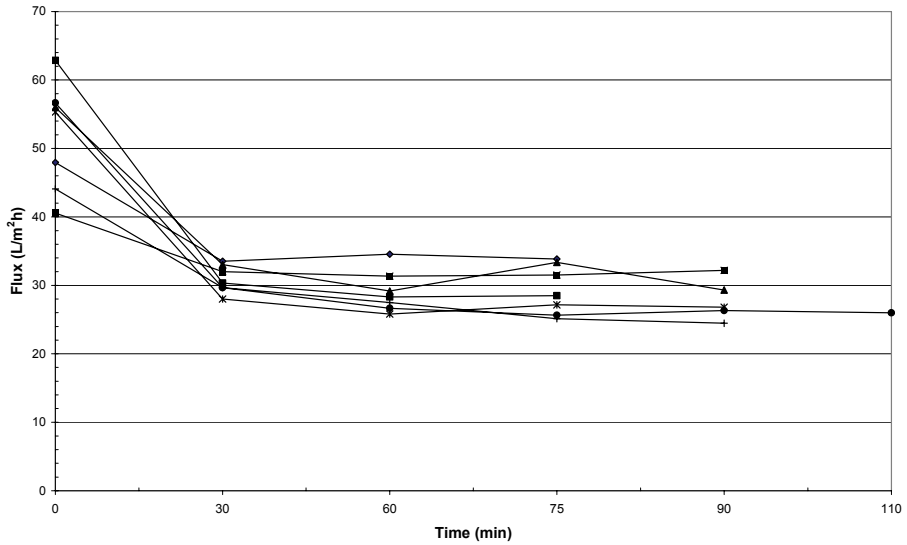

Figure 24: Membrane process flux measured for the duration of 7 different concentration cycles of the HRP solutions. The same membrane module was used for all repeat concentration runs after thorough chemical cleaning.

The unused membrane produced the shortest period needed to concentrate the HRP solution by a factor of 5. Thereafter, each concentration run using a fresh HRP solution tended to take longer to achieve the same degree of concentration for the HRP solution. Start-up flux values following each chemical cleaning procedure fluctuated but gradual stabilization is observed from the data in Figure 24. Flux values for the HRP solutions decrease after each consecutive

concentration cycle although the final three runs indicate that a degree of stabilization had occurred.

This fluctuating pattern of flux values for the HRP concentration test show the sharp initial decline of flux followed by a longer period of slow decline in flux. After the chemical procedures a sharp rise in flux is observed at the start of each new protein concentration run. The duration of HRP concentration gradually increases and the flux values obtained at the start and end of each run tend to be lower than similar values for the previous run. However, when one analyses the data in Figure 25, one can see a slow decline in process and start-up flux with time. This is indicative of adsorptive fouling which the chemical cleaning regime used was incapable of restoring. In order to restore the flux loss to the original value, a much harsher cleaning protocol has to be used. The membranes used were unhydrophilized capillary PSU membranes.

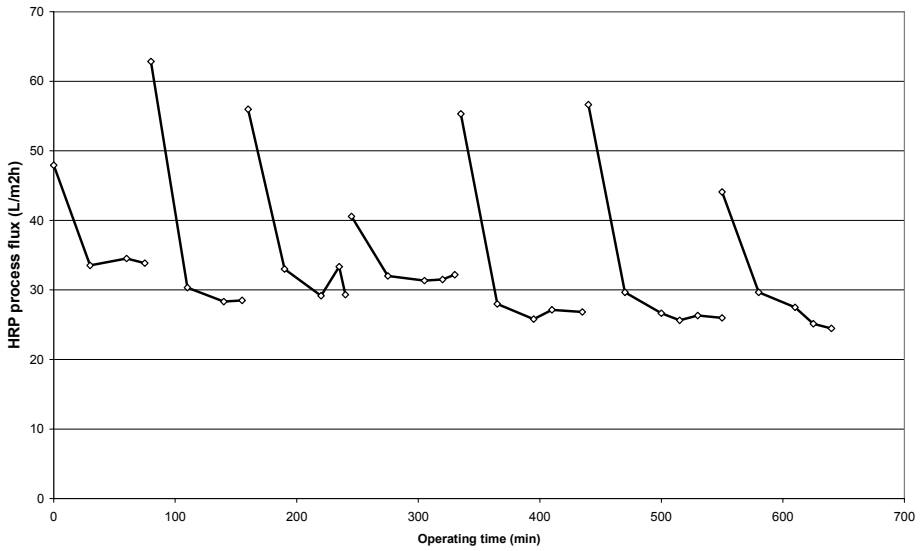

Figure 25: The flux data of successive HRP concentration cycles (same data as in Figure 24). These runs were performed with the same membrane module and the duration of this evaluation is indicated in minutes.

4. Conclusions

Development of hydrophilic, non-fouling, UF membranes by means of in-situ coating of existing membranes were abandoned because of the associated loss in membrane flux.
Branched block copolymers containing pluronic and PEO (hydrophilic) segments were successfully synthesized in small quantities using specialised laboratory equipment. Much larger quantities of these copolymers were successfully synthesized.

By incorporating the branched block copolymers into the membrane casting solutions, membrane films and flat-sheet UF membranes with a more hydrophilic character were successfully fabricated.

Unmodified UF membranes were developed and evaluated regarding flux, selectivity and fouling, using HRP protein solutions as feed.

The modification technique described in this report is suitable for use in UF membrane manufacturing. The main advantage of this technique is the ease of incorporating the modifying copolymer into membrane casting solutions by simple blending.

5. Future research

Further research regarding the effects on membrane morphology and pore size following the addition of the membrane modifying copolymer remains a priority. More complete control regarding membrane flux and selectivity will allow flexibility in manufacturing UF membranes optimised for specific feed solutions. Improving the flux characteristics of this type of capillary membranes without compromising the selectivity of these hydrophilic modified membranes could be vital in reducing costs associated with membrane technology.
The effects of chemical cleaning procedures on the stability and longevity of hydrophilic modifying groups on the membrane surface in harsh chemical environments and over long periods of normal membrane plant operations, including chemical cleaning actions, must be determined.

Additional research to further reduce the degree of hydrophilization of this type of membrane may be important in producing membranes capable of effective and long-term oil/water separation applications.

The *de novo* synthesis of polymers to produce amphiphilic copolymers allowing both structural integrity and surface modification properties already plays an important role in biotechnology regarding the development of artificial arteries and organs. Further development of the technology described in this report may have a significant impact in this field.

6. References

[1] LF Hancock, SM Fagan and MS Ziolo, (2000) Hydrophylic, semipermeable membranes fabricated with poly(ethylene oxide)-polysulfone block copolymer, Biomaterials 21, 725-733.

[2] JA Koehler, M Ulbricht and G Belfort, (2000) Intermolecular Forces between a Protein and a Hydrophylic Modified Polysulfone Film with Relevance to Filtration, Langmuir 16, 10419-1-427.

[3] SP Nunes, ML Sforça and K-V Peinemann, (1995) Dense hydrophilic composite membranes for ultrafiltration, Journal of Membrane Science 106, 49-56.

[4] ML Steen, L Hymas, ED Havey, NE Capps, DG Castner and ER Fischer, (2001) Low temperature plasma treatment of asymmetric polysulfone membranes for permanent hydrophilic surface modification, Journal of Membrane Science 188 97-114.

[5] LF Hancock, (1997) Phase Inversion Membranes with an Organized Surface Structure from Mixtures of Polysulfone and Polysulfone-Poly(ethylene oxide) Block Copolymers, Journal of Applied Polymer Science 66, 1353-1358.

[6] LF Hancock and SM Fagan, (2001) Highly Branched Block Copolymers, US Patent 6,172,180 B1.

[7] HU Bergmeyer, (1974) Methods of Enzymatic Analysis 1, 495, 2nd edition, Academic Press, New York.

[8] Yuan-Ping Ting, LF Hancock, (1996) Preparation of polysulphone /poly(ethylene oxide) block copolymers, Macromolecules 29, 7619-7621.

[9] LF Hancock, (1997) Phase Inversion Membranes with an Organized Surface Structure from Mixtures of Polysulfone and Polysulfone-Poly(ethylene oxide) Block Copolymers, Journal of Applied Polymer Science 66, 1353-1358.

[10] P van de Witte, PJ Dijkstra, JWA van den Berg and J Feijen, (1996) Phase separation processes in polymer solutions in relation to membrane formation, Journal of Membrane Science 117, 1-31.

[11] Myeong-Jin Han and Suk-Tae Nam, (2002) Thermodynamic and rheological variation in polysulphone solution by PVP and its effect in the preparation of phase inversion membrane, Journal of Membrane Science 202, 55-61.

[12] Hyuck Jai Lee, J Won, H Lee and YS Kang, (2002) Solution properties of poly(amic acid)-NMP containing LiCl and their effects on membrane morphologies, Journal of Membrane Science 196, 267-277.

[13] P Radovanovic, WT Thiel and Sun-Tak Hwang, (1992) Formation of asymmetric polysulfone membranes by immersion precipitation. Part II. The effects of casting solution and gelation bath compositions on membrane structure and skin formation, Journal of Membrane Science 65, 231-246.

[14] JY Kim, HK Lee and SC Kim, (1999) Surface structure and phase separation mechanism of polysulphone membranes by atomic force microscopy, Journal of Membrane Science 163, 159-166.

[15] SR Kim, KH Lee, and MS Jhon, (1996) The effect of ZnCl2 on the formation of polysulphone membrane, *Journal of Membrane Science* 119, 59-64.

[16] A Weisenhorn, P Maivald, H Butt, P Hansma, Physical Review B, 45, (1992) 11226-11232.

[17] H Krotil, T Stifter, H Waschipky, K Weishaupt, S Hild, O Marti, Surface and Interface Analysis, 27, (1999) 336-340.

[18] O Marti, T Stifter, H Waschipky, M Quintus, S Hild, Colloids and Surfaces, 154, (1999) 65-73.

[19] CD Frisbie, LF Rozsnyai, A Noy, MS Wrighton, CM Lieber, Science, 265, (1994) 2071-2074.

[20] S Akari, D Horn, H Keller, Advanced Materials, 7, (1995) 549-551.

[21] P Spitzig, PhD thesis, University of Ulm, 2002.

[22] F Sato, H Okui, U Akiba, K Suga, M Fujihira, Ultramicroscopy, 97, (2003) 303-314.

[23] Y Okabe, U Akba, M Fujihira, Applied Surface Science, 157, (2000) 398-404.

[24] Witec, manual, version 2.0 (2003).

[25] Nanoworld, product guide, (2002).

[26] DY Kwock, C Lam, A Li, A Leung, R Wu, E Mok, AW Neumann, Measuring and interpreting contact angles: a complex issue, Colloids and Surfaces A, 142 (1998), 219.

[27] AW Adamson, Physical chemistry of surfaces, Interscience Publishers New York (1960).

[28] IH Huisman, et al., The effect of protein-protein and protein-membrane interactions on membrane fouling in ultrafiltration, Journal of Membrane Science, 179 (2000), 79.

[29] MA Yakup, M Yilmaz, E Yalcin, G Bayramoglu, Affinity membrane chromatography, Journal of Chromatography B, 805 (2004), 315.

[30] P van de Witte, PJ Dijkstra, J van den Berg, J Feijen, Phase separation process in polymer solutions in relation to membrane formation, Journal of Membrane Science, 117 (1996), 1.

[31] MJ Han, D Bhattacharyya, Changes in morphology and transport characteristics of polysulfone membranes prepared by different demixing conditions, Journal of Membrane Science, 98 (1995), 191

[32] JH Kim, KH Lee, Effect of PEG additive on membrane formation by phase inversion, Journal of Membrane Science, 138 (1998),153.

[33] HJ Lee, J Won, H Lee, YS Kang, Solution properties of poly(amic acid)-NMP containing LiCl and their effects on membrane morphologies, Journal of Membrane Science, 196 (2002), 267-277

Technology transfer

Dissemination of results

Oral and poster presentations at Conferences or Symposia

Surface analysis of ultrafiltration membranes using AFM, M Meincken, SP Roux, MSSA conference, Pietermaritzburg, December 5-8, 2005, (accepted for oral presentation).

Hydrophilization of capillary ultrafiltration membranes with the use of a branched poly(ethylene oxide)-block-polysulphone copolymer, SP Roux, EP Jacobs, AJ van Reenen, C Morkel, M Meincken, 6th WISA-MTD Workshop, Wilderness, South Africa, 13-15 March 2005.

Analysis of poly(ethyleneglycol-styrene) block copolymers by 2D-chromatography, V Grumel, AJP van Zyl, CE Morkel, AJ Van Reenen, 17th International Symposium for Polymer Analysis and Characterization, ISPAC-2004, Heidelberg, Germany, 7-9 Jun 2004

*A*nalysis of poly(ethyleneglycol-styrene) block copolymers by 2D chromatography, V Grumel, AJP van Zyl, CE Morkel, AJ van Reenen, CIMM Conference on Materials & Manufacturing Technology Together, University of Cape Town, Cape Town, 14-15 October 2004.

Publications

Accepted or In press

Hydrophilization of polysulphone ultrafiltration membranes by incorporation of branched PEO-block-PSU copolymers, SP Roux, EP Jacobs, AJ van Reenen, C Morkel and M Meincken, J of Membrane Science (2005).

A new approach to quantify the hydrophilic character of membranes by pulsed force mode atomic force microscopy, M Meincken, SP Roux, EP Jacobs, *Applied Surface Science* (2005), Available on-line.

Post-graduate studies

Research in progress

Hydrophilization of capillary UF membranes, SP Roux, PhD-study.

Theses accepted

The synthesis and characterization of amphiphilic clock copolymers, CE Morkel, PhD-thesis, University of Stellenbosch, 2005.